Electronic Transactions on Numerical Analysis.
Volume 41, pp. 306-327, 2014.

ISSN 1068-9613.

ETNA
Kent State University
http://etna.math.kent.edu

FINITE ELEMENT APPROXIMATION OF VISCOELASTIC FLOW IN A MOVING DOMAIN*

JASON HOWELL†, HYESUK LEE‡, AND SHUHAN XU‡

Abstract. In this work the problem of a viscoelastic fluid flow in a movable domain is considered. A numerical approximation scheme is developed based on the Arbitrary Lagrangian-Eulerian (ALE) formulation of the flow equations. The spatial discretization is accomplished by the finite element method, and the discontinuous Galerkin method is used for stress approximation. Both first and second order time-stepping schemes satisfying the geometric conservation law (GCL) are derived and analyzed, and numerical experiments that support the theoretical results are presented.

Key words. Viscoelastic fluid flow, moving boundary, finite elements, fluid-structure interaction.

AMS subject classifications. 65M60, 65M12.

1. Introduction.

In this paper we consider a viscoelastic fluid flow problem posed in a moving spatial domain. Such problems arise in modeling the interaction of fluid flows with an elastic medium, which is of great interest in many industrial and biomechanical applications, including the flow of blood in medium-to-large arteries. In such situations, the physical problem of interest exhibits significant two-way interaction between the fluid and the solid structure. The accurate and efficient computer simulation of such fluid-structure interaction (FSI) problems is of paramount importance to researchers working in these applications, and much effort is dedicated to producing good algorithms [8, 28, 34, 37, 40].

Motivation for the work presented here stems from recent advances in computing Newtonian and quasi-Newtonian fluid flows in moving domains, including methods designed for fluid motion within deformable elastic structures. The fluid equations and structure equations are most commonly posed from different perspectives in continuum mechanics: the Eulerian frame of reference for the fluid equations and the Lagrangian frame of reference for elastic structures. With this discrepancy in mind, the Arbitrary Lagrangian-Eulerian (ALE) method was developed in the 1980s to allow for the coupled fluid-structure problem to be posed in a single framework [11, 24]. In [32], Nobile employed the ALE formulation to first derive methods for a Newtonian fluid flow governed by the Navier-Stokes equations in a moving domain, and then coupled this formulation with an elastic structure. Several subsequent works discuss different aspects of the Newtonian fluid-structure interaction problem, including boundary conditions [13, 14, 33], numerical stability [7, 14], and fixed-point methods for the coupled fluid-structure problem [10]. Other researchers have also shown convergence results for the ALE formulation of the Stokes problem [30], and other related problems [1, 19].

However, many industrial and biological fluids of considerable interest do not behave as Newtonian fluids. One example of great interest is blood. The study of *hemodynamical flows* yields constitutive models that are non-Newtonian in nature, exhibiting both shear-thinning and viscoelastic behavior [17, 20, 41]. Several recent investigations show that the non-Newtonian characteristics of blood can have significant impact on the characteristics of blood flow [3, 4, 25, 29, 31], and algorithms that capture the behavior of such non-Newtonian fluids in moving domains and deformable elastic structures are desirable. There are existing works which derive and implement numerical methods for simulation of such problems,

*Received September 1, 2012. Accepted April 29, 2014. Published online on October, 6, 2014. Recommended by S. Brenner.
†Department of Mathematics, College of Charleston, Charleston, SC 29424 (howelljs@cofc.edu).
‡Department of Mathematical Sciences, Clemson University, Clemson, SC 29634-0975 ({hklee,shuhanx}@clemson.edu).

ETNA
Kent State University
http://etna.math.kent.edu

including those employing the ALE approach [25, 29], hybrid finite element/finite volume approaches [31], and the immersed boundary method [9, 39]. However, a detailed numerical analysis, including theoretical stability results for time-stepping schemes, of such methods applied to non-Newtonian problems is, in general, lacking from the current literature.

In [27], Lee investigated numerical approximation of an unsteady flow problem governed by a quasi-Newtonian model in a moving domain, where a boundary velocity is given by a known function. A variational formulation of the problem by the Arbitrary Lagrange Eulerian method was derived and a priori error estimates for the semi-discrete and fully discrete ALE formulations were obtained. Lee also examined several temporal discretization schemes for stability and accuracy, where the theoretical results were supported by numerical tests.

In the same spirit as [27], the objective of the work presented here is to develop and analyze a finite element method for the time-dependent Johnson-Segalman viscoelastic fluid flow model (of which the Oldroyd-B model is a special case) set in a movable domain. This work serves as an intermediate step between the aforementioned works and the development and verification of algorithms for the simulation of a viscoelastic fluid in a deformable elastic structure, and the extension of that to the shear-thinning viscoelastic case. Specifically, the problem is posed in a moving spatial domain, and the ALE formulation of the conservation equations is utilized to pose the equations in a reference domain. The spatial discretization is accomplished via the finite element method, and we employ discontinuous approximations for the fluid stress. First and second-order time-stepping schemes satisfying the geometric conservation law (GCL) are derived, and theoretical stability results are shown.

This paper is organized as follows. In Section 2, we describe the model problem and introduce an ALE formulation. We consider finite element approximations of the ALE formulation in Section 3 and in Section 4 time discretization schemes are discussed and analyzed. Finally, we present numerical results in Section 5 that support the theoretical results and exhibit stability of the algorithms developed here. Concuding remarks can be found in Section 6.

2. Model equations and ALE formulation. Let Ω_t be a bounded domain at time t in $\mathbb{R}^2$ with the Lipschitz continuous boundary Γ_t, where Γ_t is a moving boundary. Movement of Γ_t is described by the boundary position function $\mathbf{h} : \Gamma_0 \times [0,T] \to \Gamma_t$ such that $\Gamma_t = \mathbf{h}(t, \Gamma_0)$. Consider the viscoelastic model equations,

$$\boldsymbol{\sigma} + \lambda \left(\frac{\partial \boldsymbol{\sigma}}{\partial t} + \mathbf{u} \cdot \nabla \boldsymbol{\sigma} + g_a(\boldsymbol{\sigma}, \nabla \mathbf{u}) \right) - 2\,\alpha\, D(\mathbf{u}) = \mathbf{0} \quad \text{in } \Omega_t\,, \tag{2.1}$$

$$\rho \left(\frac{\partial \mathbf{u}}{\partial t} + \mathbf{u} \cdot \nabla \mathbf{u} \right) - \nabla \cdot \boldsymbol{\sigma} - 2(1-\alpha)\, \nabla \cdot D(\mathbf{u}) + \nabla p = \mathbf{f} \quad \text{in } \Omega_t\,, \tag{2.2}$$

$$div\ \mathbf{u} = 0 \quad \text{in } \Omega_t\,, \tag{2.3}$$

where $\boldsymbol{\sigma}$ denotes the extra stress tensor, $\mathbf{u}$ the velocity vector, p the pressure of the fluid, ρ the density of the fluid, and λ is the Weissenberg number defined as the product of the relaxation time and a characteristic strain rate. Assume that p has zero mean value over Ω_t. In (2.1) and (2.2), $D(\mathbf{u}) := (\nabla \mathbf{u} + \nabla \mathbf{u}^T)/2$ is the rate of the strain tensor, α a number such that $0 < \alpha < 1$ which may be considered as the fraction of viscoelastic viscosity, and $\mathbf{f}$ the body force. In (2.1), $g_a(\boldsymbol{\sigma}, \nabla \mathbf{u})$ is defined by

$$g_a(\boldsymbol{\sigma}, \nabla \mathbf{u}) := \frac{1-a}{2}(\boldsymbol{\sigma} \nabla \mathbf{u} + \nabla \mathbf{u}^T \boldsymbol{\sigma}) - \frac{1+a}{2}(\nabla \mathbf{u}\, \boldsymbol{\sigma} + \boldsymbol{\sigma} \nabla \mathbf{u}^T)$$

for $a \in [-1, 1]$. Note that (2.1) reduces to the Oldroyd-B model for the case $a = 1$.

ETNA
Kent State University
http://etna.math.kent.edu

Initial and boundary conditions for $\mathbf{u}$ and $\boldsymbol{\sigma}$ are given as follows:

$$\mathbf{u}(\mathbf{x},0) = \mathbf{u}^0 \quad \text{in } \Omega_0\,,$$

$$\boldsymbol{\sigma}(\mathbf{x},0) = \boldsymbol{\sigma}^0 \quad \text{in } \Omega_0\,,$$

$$\mathbf{u} = \mathbf{u}_{BC} \quad \text{on } \Gamma_t\,,$$

$$\boldsymbol{\sigma} = \boldsymbol{\sigma}_{BC} \text{ on } \Gamma_{tin},$$

where $\int_{\Gamma_t} \mathbf{u}_{BC} \cdot \mathbf{n}\, d\Gamma_t = 0$ and Γ_{tin} is the inflow boundary.

In the present paper, the constitutive equation (2.1) is slightly modified for numerical analysis of the governing equations. It is well known that the g_a term in the constitutive equation presents a difficulty when analyzing viscoelastic flow equations. Therefore, we will consider a nearby problem in which the g_a term is linearized with the given velocity $\mathbf{b}(\mathbf{x})$:

$$\boldsymbol{\sigma} + \lambda \left(\frac{\partial \boldsymbol{\sigma}}{\partial t} + \mathbf{u} \cdot \nabla \boldsymbol{\sigma} + g_a(\boldsymbol{\sigma}, \nabla \mathbf{b}) \right) - 2\,\alpha\, D(\mathbf{u}) = \mathbf{0} \quad \text{in } \Omega_t\,, \tag{2.4}$$

for the constitutive equation, where the following assumption is made for $\mathbf{b}$:

$$\mathbf{b} \in \mathbf{H}^1(\Omega_t), \qquad \nabla \cdot \mathbf{b} = 0, \qquad \|\mathbf{b}\|_\infty \le M, \qquad \|\nabla \mathbf{b}\|_\infty \le M\,.$$

It should be noted that the flow here is not assumed to be creeping (i.e., slow) as in [12]. Therefore, the convective term $\mathbf{u} \cdot \nabla \mathbf{u}$ is retained in the momentum equation (2.2). We also assume the homogeneous boundary condition for the stress function, i.e., $\boldsymbol{\sigma}_{BC} = \mathbf{0}$ to simplify the analysis. The non-homogeneous case, $\boldsymbol{\sigma}_{BC} \neq \mathbf{0}$, can be treated in the similar way for the non-homogeneous velocity boundary condition. In the application of a fluid-structure interaction system, the inflow part on the moving boundary changes from time to time. This is due to an interface condition, which makes numerical studies of the system extremely challenging, not only due to the change of inflow boundaries, but also because of a lack of boundary information on the stress. There are several different ways suggested to implement a stress boundary condition in the literature. One possible way would be to compute the boundary value of stress using velocity information as given in [18] and use this as a stress condition for the next (time or sub-) iteration.

We use the Sobolev spaces $W^{m,p}(D)$ with norms $\|\cdot\|_{m,p,D}$ if $p < \infty$, $\|\cdot\|_{m,\infty,D}$ if $p = \infty$. Denote the Sobolev space $W^{m,2}$ by H^m with the norm $\|\cdot\|_{m,D}$. The corresponding space of vector-valued or tensor-valued functions is denoted by $\mathbf{H}^m$.

The Arbitrary Lagrangian Eulerian (ALE) [11] method is one of the most widely used numerical schemes for simulating fluid flows in a moving domain. In the ALE formulation, a one-to-one coordinate transformation is introduced for the fluid domain, and the fluid equations can be rewritten with respect to a fixed reference domain. Specifically, we define the time-dependent bijective mapping Ψ_t which maps the reference domain Ω_0 to the physical domain Ω_t:

$$\Psi_t : \Omega_0 \to \Omega_t, \qquad \Psi_t(\mathbf{y}) = \mathbf{x}(\mathbf{y}, t)\,,$$

where $\mathbf{y}$ and $\mathbf{x}$ are the spatial coordinates in Ω_0 and Ω_t, respectively. The coordinate $\mathbf{y}$ is often called the *ALE coordinate*. Using Ψ_t, the weak formulation of the flow equations in Ω_t can be recast into a weak formulation defined in the reference domain Ω_0. Thus the model equations in the reference domain can be considered for numerical simulation and the transformation function Ψ_t needs to be determined at each time step as a part of the computations.

ETNA
Kent State University
http://etna.math.kent.edu

For a function $\phi : \Omega_t \times [0,T] \to \mathbb{R}$, its corresponding function $\overline{\phi} = \phi \circ \Psi_t$ in the ALE setting is defined as

$$\overline{\phi} : \Omega_0 \to \mathbb{R}, \qquad \overline{\phi}(\mathbf{y},t) = \phi(\Psi_t(\mathbf{y}),t).$$

The time derivative in the ALE frame is also given as

$$\frac{\partial \phi}{\partial t}\,|_{\mathbf{y}} \colon \Omega_t \times [0,T] \to \mathbb{R}, \qquad \frac{\partial \phi}{\partial t}\,|_{\mathbf{y}}\,(\mathbf{x},t) = \frac{\partial \overline{\phi}}{\partial t}(\mathbf{y},t).$$

Using the chain rule, we have

$$\frac{\partial \phi}{\partial t}\,|_{\mathbf{y}} = \frac{\partial \phi}{\partial t}\,|_{\mathbf{x}} + \mathbf{w} \cdot \nabla_{\mathbf{x}} \phi, \tag{2.5}$$

where $\mathbf{w} := \frac{\partial \mathbf{x}}{\partial t}\,|_{\mathbf{y}}$ is the domain velocity. In (2.5), $\frac{\partial \phi}{\partial t}\,|_{\mathbf{y}}$ is the so-called *ALE derivative* of ϕ. The flow equations (2.2), (2.3) and (2.4) can be then written in the ALE formulation as

$$\boldsymbol{\sigma} + \lambda \left(\frac{\partial \boldsymbol{\sigma}}{\partial t}\,|_{\mathbf{y}} + (\mathbf{u}-\mathbf{w}) \cdot \nabla_{\mathbf{x}} \boldsymbol{\sigma} + g_a(\boldsymbol{\sigma}, \nabla_{\mathbf{x}} \mathbf{b}) \right) - 2\,\alpha\, D_{\mathbf{x}}(\mathbf{u}) = \mathbf{0} \quad \text{in } \Omega_t\,, \tag{2.6}$$

$$\rho \left(\frac{\partial \mathbf{u}}{\partial t}\,|_{\mathbf{y}} + (\mathbf{u}-\mathbf{w}) \cdot \nabla_{\mathbf{x}} \mathbf{u} \right) - \nabla_{\mathbf{x}} \cdot \boldsymbol{\sigma} - 2(1-\alpha)\,\nabla_{\mathbf{x}} \cdot D_{\mathbf{x}}(\mathbf{u}) + \nabla_{\mathbf{x}} p = \mathbf{f} \quad \text{in } \Omega_t\,, \tag{2.7}$$

$$\nabla_{\mathbf{x}} \cdot \mathbf{u} = 0 \quad \text{in } \Omega_t\,, \tag{2.8}$$

where $D_{\mathbf{x}}(\mathbf{u}) = (\nabla_{\mathbf{x}} \mathbf{u} + \nabla_{\mathbf{x}} \mathbf{u}^T)/2$. Note that all spatial derivatives involved in (2.6)–(2.8), including the divergence operator, are with respect to $\mathbf{x}$. Throughout the paper we will use $D_{\mathbf{x}}(\cdot)$ and $\nabla_{\mathbf{x}}$ only when they need to be clearly specified. Otherwise, $D(\cdot)$, ∇ will be used as $D_{\mathbf{x}}(\cdot)$, $\nabla_{\mathbf{x}}$, respectively.

For the variational formulation of the flow equations (2.6)–(2.8) in the ALE framework, define function spaces for the reference domain:

$$\begin{aligned}
&\mathbf{U}_0 := \mathbf{H}_0^1(\Omega_0)\,,\\
&Q_0 := L_0^2(\Omega_0) = \{\overline{q} \in L^2(\Omega_0) : \ \textstyle\int_{\Omega_0} \overline{q}\, d\Omega = 0\}\,,\\
&\boldsymbol{\Sigma}_0 := \{\boldsymbol{\tau} \in \mathbf{L}^2(\Omega_0) : \tau_{ij} = \tau_{ji},\ \boldsymbol{\tau} = \mathbf{0} \text{ on } \Gamma_{tin},\ (\mathbf{b}\cdot\nabla)\boldsymbol{\tau} \in \mathbf{L}^2(\Omega_0)\}\,.
\end{aligned}$$

The function spaces for Ω_t are then defined as

$$\begin{aligned}
&\mathbf{U}_t := \{\mathbf{v} : \Omega_t \times [0,T] \to \mathbb{R}^2,\ \mathbf{v} = \overline{\mathbf{v}} \circ \Psi_t^{-1} \text{ for } \overline{\mathbf{v}} \in \mathbf{U}_0\}\,,\\
&Q_t := \{q : \Omega_t \times [0,T] \to \mathbb{R},\ q = \overline{q} \circ \Psi_t^{-1} \text{ for } \overline{p} \in Q_0\}\,,\\
&\boldsymbol{\Sigma}_t := \{\boldsymbol{\tau} : \Omega_t \times [0,T] \to \mathbb{R}^{2\times 2},\ \boldsymbol{\tau} = \overline{\boldsymbol{\tau}} \circ \Psi_t^{-1} \text{ for } \overline{\boldsymbol{\tau}} \in \boldsymbol{\Sigma}_0\}\,.
\end{aligned}$$

If the ALE mapping Ψ_t satisfies the regularity conditions [15, 21, 30]

$$\Psi_t \in \mathbf{W}^{2,\infty}(\Omega_t), \qquad \Psi_t^{-1} \in \mathbf{W}^{2,\infty}(\Omega_t),$$

then

$$(\mathbf{v}, q, \boldsymbol{\tau}) \in \mathbf{U}_t \times Q_t \times \boldsymbol{\Sigma}_t \iff (\overline{\mathbf{v}}, \overline{q}, \overline{\boldsymbol{\tau}}) = (\mathbf{v} \circ \Psi_t, q \circ \Psi_t, \boldsymbol{\tau} \circ \Psi_t) \in \mathbf{U}_0 \times Q_0 \times \boldsymbol{\Sigma}_0\,. \tag{2.9}$$

ETNA
Kent State University
http://etna.math.kent.edu

Based on the regularity condition of the ALE function (2.9), we assume that the domain velocity is bounded, i.e.,

$$\|\mathbf{w}\|_{1,\Omega_t} < C \tag{2.10}$$

for $C > 0$.

For given $\mathbf{u}_{BC} \in \mathbf{H}^{1/2}(\Gamma_t)$, there exists $\mathbf{u}^* \in \mathbf{H}^1(\Omega_t)$ such that

$$\mathbf{u}^*|_{\Gamma_t} = \mathbf{u}_{BC}, \qquad \nabla \cdot \mathbf{u}^* = 0$$

and

$$|(\mathbf{v} \cdot \nabla \mathbf{u}^*, \mathbf{v})| \le \epsilon \|\mathbf{v}\|_1^2 \quad \forall \mathbf{v} \in \mathbf{U}_t \tag{2.11}$$

for any $\epsilon > 0$ [38]. Writing the velocity function as $\mathbf{u} = \widetilde{\mathbf{u}} + \mathbf{u}^*$, we have $\widetilde{\mathbf{u}}|_{\Gamma_t} = \mathbf{0}$, $\nabla \cdot \widetilde{\mathbf{u}} = 0$ and the variational formulation for $(\widetilde{\mathbf{u}}, p, \boldsymbol{\sigma})$ in the ALE framework is given by: find $(\widetilde{\mathbf{u}}, p, \boldsymbol{\sigma})$ such that

$$\begin{aligned}(\boldsymbol{\sigma},\, \boldsymbol{\tau})_{\Omega_t} + \lambda \left(\frac{\partial \boldsymbol{\sigma}}{\partial t} \,|_{\mathbf{y}} + ((\widetilde{\mathbf{u}} + \mathbf{u}^* - \mathbf{w}) \cdot \nabla)\boldsymbol{\sigma} + g_a(\boldsymbol{\sigma}, \nabla \mathbf{b}),\, \boldsymbol{\tau} \right)_{\Omega_t} \\ - 2\alpha\,(D(\widetilde{\mathbf{u}}),\, \boldsymbol{\tau})_{\Omega_t} = 2\alpha\,(D(\mathbf{u}^*),\, \boldsymbol{\tau})_{\Omega_t} \quad \forall \boldsymbol{\tau} \in \boldsymbol{\Sigma}_t\,,\end{aligned} \tag{2.12}$$

$$\begin{aligned}&\rho \left(\frac{\partial \widetilde{\mathbf{u}}}{\partial t} \,|_{\mathbf{y}} + (\widetilde{\mathbf{u}} - \mathbf{w}) \cdot \nabla \widetilde{\mathbf{u}} + \widetilde{\mathbf{u}} \cdot \nabla \mathbf{u}^* + \mathbf{u}^* \cdot \nabla \widetilde{\mathbf{u}},\, \mathbf{v} \right)_{\Omega_t} + (\boldsymbol{\sigma}, D(\mathbf{v}))_{\Omega_t} \\ &\qquad + 2(1-\alpha)(D(\widetilde{\mathbf{u}}), D(\mathbf{v}))_{\Omega_t} - (p, \nabla \cdot \mathbf{v})_{\Omega_t} \\ &= (\mathbf{f}, \mathbf{v})_{\Omega_t} - \rho \left(\frac{\partial \mathbf{u}^*}{\partial t} \,|_{\mathbf{y}} + (\mathbf{u}^* - \mathbf{w}) \cdot \nabla \mathbf{u}^*, \mathbf{v} \right)_{\Omega_t} \\ &\qquad - 2(1-\alpha)(D(\mathbf{u}^*), D(\mathbf{v}))_{\Omega_t} \;\forall \mathbf{v} \in \mathbf{U}_t\,,\end{aligned} \tag{2.13}$$

$$(q, \nabla \cdot \widetilde{\mathbf{u}})_{\Omega_t} = 0 \quad \forall q \in Q_t\,. \tag{2.14}$$

Using integration by parts, $\nabla \cdot \widetilde{\mathbf{u}} = 0$ and $\widetilde{\mathbf{u}}\,|_{\Gamma_t} = 0$, the convective terms in (2.12)–(2.13) can be written as

$$\begin{aligned}((\widetilde{\mathbf{u}} - \mathbf{w}) \cdot \nabla)\boldsymbol{\sigma}, \boldsymbol{\sigma})_{\Omega_t} &= \frac{1}{2}\left[((\nabla \cdot \mathbf{w})\boldsymbol{\sigma}, \boldsymbol{\sigma})_{\Omega_t} - ((\mathbf{w} \cdot \mathbf{n})\boldsymbol{\sigma}, \boldsymbol{\sigma})_{\Gamma_t}\right]\,, \\ ((\widetilde{\mathbf{u}} - \mathbf{w}) \cdot \nabla)\widetilde{\mathbf{u}}, \widetilde{\mathbf{u}})_{\Omega_t} &= \frac{1}{2}((\nabla \cdot \mathbf{w})\widetilde{\mathbf{u}}, \widetilde{\mathbf{u}})_{\Omega_t}\,.\end{aligned}$$

Note that if $\mathbf{w} = 0$,

$$(\widetilde{\mathbf{u}} \cdot \nabla \boldsymbol{\sigma}, \boldsymbol{\sigma})_{\Omega_t} = 0, \qquad (\widetilde{\mathbf{u}} \cdot \nabla \widetilde{\mathbf{u}}, \widetilde{\mathbf{u}})_{\Omega_t} = 0\,.$$

In order to simplify expressions, throughout this paper we will use the bilinear form A_t defined by

$$\begin{aligned}A_t((\widetilde{\mathbf{u}}, \boldsymbol{\sigma}), (\mathbf{v}, \boldsymbol{\tau})) := (\boldsymbol{\sigma},\, \boldsymbol{\tau})_{\Omega_t} + \lambda\,(g_a(\boldsymbol{\sigma}, \nabla \mathbf{b}),\, \boldsymbol{\tau})_{\Omega_t} - 2\alpha\,(D(\widetilde{\mathbf{u}}),\, \boldsymbol{\tau})_{\Omega_t} \\ + 2\alpha\,(\boldsymbol{\sigma},\, D(\mathbf{v}))_{\Omega_t} + 4\alpha(1-\alpha)\,(D(\widetilde{\mathbf{u}}),\, D(\mathbf{v}))_{\Omega_t}\,.\end{aligned} \tag{2.15}$$

Since

$$(g_a(\boldsymbol{\sigma}, \nabla \mathbf{b}), \boldsymbol{\tau})_{\Omega_t} \le 4\|\nabla \mathbf{b}\|_{\infty,\Omega_t}\|\boldsymbol{\sigma}\|_{0,\Omega_t}\|\boldsymbol{\tau}\|_{0,\Omega_t} \le 4M\,\|\boldsymbol{\sigma}\|_{0,\Omega_t}\|\boldsymbol{\tau}\|_{0,\Omega_t}\,,$$

ETNA
Kent State University
http://etna.math.kent.edu

we have, using the Poincaré inequality $\|D(\widetilde{\mathbf{u}})\|_{0,\Omega_t} \geq C_p\|\widetilde{\mathbf{u}}\|_{1,\Omega_t}$,

$$\begin{aligned} A_t((\widetilde{\mathbf{u}},\boldsymbol{\sigma}),(\widetilde{\mathbf{u}},\boldsymbol{\sigma})) &\geq (1-4\lambda M)\,\|\boldsymbol{\sigma}\|^2_{0,\Omega_t} + 4\alpha(1-\alpha)\|D(\widetilde{\mathbf{u}})\|^2_{0,\Omega_t} \\ &\geq (1-4\lambda M)\,\|\boldsymbol{\sigma}\|^2_{0,\Omega_t} + 4\alpha(1-\alpha)C_p^2\|\widetilde{\mathbf{u}}\|^2_{1,\Omega_t} \end{aligned} \tag{2.16}$$

and

$$\begin{aligned} A_t((\boldsymbol{\sigma},\widetilde{\mathbf{u}}),(\boldsymbol{\tau},\mathbf{v})) &\leq (1+4\lambda M)\,\|\boldsymbol{\sigma}\|_{0,\Omega_t}\|\boldsymbol{\tau}\|_{0,\Omega_t} + 2\alpha\|D(\widetilde{\mathbf{u}})\|_{0,\Omega_t}\|\boldsymbol{\tau}\|_{0,\Omega_t} \\ &\quad +2\alpha\|\boldsymbol{\sigma}\|_{0,\Omega_t}\|D(\mathbf{v})\|_{0,\Omega_t} + 4\alpha(1-\alpha)\|D(\widetilde{\mathbf{u}})\|_{0,\Omega_t}\|D(\mathbf{v})\|_{0,\Omega_t} \\ &\leq C(\|\boldsymbol{\sigma}\|_{0,\Omega_t} + \|\widetilde{\mathbf{u}}\|_{1,\Omega_t})(\|\boldsymbol{\tau}\|_{0,\Omega_t} + \|\mathbf{v}\|_{1,\Omega_t})\,. \end{aligned}$$

Therefore, A_t is coercive and continuous if $\lambda\, M$ is small so that $1-4\lambda M > 0$. This would be the case when the ratio of a time scale for the fluid memory to a time scale of the flow is small and the fluid has a small effect of elasticity.

A variational formulation called a *conservative form* [32] is derived based on the fact that the test function space can be mapped into a time-independent space using Ψ_t^{-1}. In order to derive a conservative variational formulation, consider the Reynolds transport formula [36]

$$\frac{d}{dt}\int_{V(t)} \phi(\mathbf{x},t)\,dV = \int_{V(t)} \frac{\partial\phi}{\partial t}\,|_{\mathbf{y}} + \phi\nabla_{\mathbf{x}}\cdot\mathbf{w}\,dV = \int_{V(t)} \frac{\partial\phi}{\partial t}\,|_{\mathbf{x}} + \mathbf{w}\cdot\nabla_{\mathbf{x}}\phi + \phi\nabla_{\mathbf{x}}\cdot\mathbf{w}\,dV$$

for a function $\phi : V(t) \to \mathbb{R}$, where $V(t) \subset \Omega_t$ such that $V(t) = \Psi_t(V_0)$ with $V_0 \subset \Omega_0$. If v is a function from Ω_t to $\mathbb{R}$ and $v = \overline{v}\circ\Psi_t^{-1}$ for $\overline{v} : \Omega_0 \to \mathbb{R}$, we have that

$$\frac{\partial v}{\partial t}\,|_{\mathbf{y}} = 0\,, \tag{2.17}$$

and therefore

$$\frac{d}{dt}\int_{\Omega_t} v\,d\Omega = \int_{\Omega_t} v\,\nabla_{\mathbf{x}}\cdot\mathbf{w}\,d\Omega\,,$$

$$\frac{d}{dt}\int_{\Omega_t} \phi v\,d\Omega = \int_{\Omega_t}\left(\frac{\partial\phi}{\partial t}\,|_{\mathbf{y}} + \phi\nabla_{\mathbf{x}}\cdot\mathbf{w}\right) v\,d\Omega\,. \tag{2.18}$$

Then, applying (2.18) to (2.12)–(2.14), we have the following variational formulation: find $(\widetilde{\mathbf{u}}, p, \boldsymbol{\sigma})$ for each $t \in (0,T]$ such that

$$\begin{aligned} &(\boldsymbol{\sigma},\boldsymbol{\tau})_{\Omega_t} + \lambda\frac{d}{dt}(\boldsymbol{\sigma},\boldsymbol{\tau})_{\Omega_t} + \lambda\Big(-\boldsymbol{\sigma}(\nabla\cdot\mathbf{w}) + ((\widetilde{\mathbf{u}}+\mathbf{u}^*-\mathbf{w})\cdot\nabla)\boldsymbol{\sigma} \\ &\qquad +g_a(\boldsymbol{\sigma},\nabla\mathbf{b}),\,\boldsymbol{\tau}\Big)_{\Omega_t} - 2\alpha(D(\widetilde{\mathbf{u}}),\boldsymbol{\tau})_{\Omega_t} = 2\alpha\,(D(\mathbf{u}^*),\,\boldsymbol{\tau})_{\Omega_t} \quad \forall\boldsymbol{\tau}\in\boldsymbol{\Sigma}_t\,, \end{aligned} \tag{2.19}$$

$$\begin{aligned} &\rho\frac{d}{dt}(\widetilde{\mathbf{u}},\mathbf{v})_{\Omega_t} + \rho\,(-\widetilde{\mathbf{u}}(\nabla\cdot\mathbf{w}) + ((\widetilde{\mathbf{u}}-\mathbf{w})\cdot\nabla)\widetilde{\mathbf{u}} + \widetilde{\mathbf{u}}\cdot\nabla\mathbf{u}^* + \mathbf{u}^*\cdot\nabla\widetilde{\mathbf{u}},\mathbf{v})_{\Omega_t} \\ &\quad +2(1-\alpha)(D(\widetilde{\mathbf{u}}),\,D(\mathbf{v}))_{\Omega_t} + (\boldsymbol{\sigma},D(\mathbf{v}))_{\Omega_t} - (p,\nabla\cdot\mathbf{v})_{\Omega_t} \\ &\quad = (\mathbf{f},\mathbf{v})_{\Omega_t} - \rho\left(\frac{\partial\mathbf{u}^*}{\partial t}\,|_{\mathbf{y}} + (\mathbf{u}^*-\mathbf{w})\cdot\nabla\mathbf{u}^*,\mathbf{v}\right)_{\Omega_t} \\ &\qquad -2(1-\alpha)(D(\mathbf{u}^*),D(\mathbf{v}))_{\Omega_t}\ \forall\mathbf{v}\in\mathbf{U}_t\,, \end{aligned} \tag{2.20}$$

$$(q,\nabla\cdot\widetilde{\mathbf{u}})_{\Omega_t} = 0 \quad \forall q\in Q_t\,. \tag{2.21}$$

ETNA
Kent State University
http://etna.math.kent.edu

The ALE weak formulation (2.19)–(2.21) is conservative in the sense that if we take a subset $V(t) \subset \Omega_t$ with Lipschitz continuous boundary, $\mathbf{f} = \mathbf{0}$ and $\mathbf{v} = constant$, then $\frac{d}{dt}\int_{V(t)} \widetilde{\mathbf{u}}\, dV$ is given in terms of boundary integrals only. Therefore, the variation of $\widetilde{\mathbf{u}}$ over $V(t)$ is due only to boundary terms [15].

In order to define the ALE mapping Ψ_t, we consider the boundary position function $h : \Gamma_0 \times [0,T] \to \Gamma_t$. The ALE mapping then may be determined by solving the Laplace equation,

$$\begin{aligned} \Delta_{\mathbf{y}}\mathbf{x}(\mathbf{y}) &= 0 \qquad \text{in } \Omega_0\,, \\ \mathbf{x}(\mathbf{y}) &= h(\mathbf{y}) \qquad \text{on } \Gamma_0\,. \end{aligned}$$

This method is called the *harmonic extension technique*, where the boundary position function h is extended onto the whole domain [15]. When the problem is posed as a fluid-structure interaction problem, other equations such as a linear elastic problem and a parabolic system also can be used to obtain the domain velocity [15, 21].

3. Finite element approximation. The spatial discretization of the viscoelastic flow problem follows that of [2]. Suppose $T_{h,0}$ is a triangulation of Ω_0 such that $\overline{\Omega}_0 = \{\cup K : K \in T_{h,0}\}$. Assume that there exist positive constants c_1, c_2 such that

$$c_1\rho_K \le h_K \le c_2\rho_K\,,$$

where h_K is the diameter of K, ρ_K is the diameter of the greatest ball included in K, and $h = \max_{K\in T_{h,0}} h_K$.

Let $P_k(K)$ denote the space of polynomials of degree less than or equal to k on $K \in T_{h,0}$. We define finite element spaces for the approximation of $(\mathbf{u}, p)$ in Ω_0:

$$\mathbf{U}_{h,0} := \{\mathbf{v} \in \mathbf{U}_0 \cap (C^0(\overline{\Omega}))^2 : \mathbf{v}|_K \in P_2(K)^2,\ \forall K \in T_{h,0}\}\,,$$

$$Q_{h,0} := \{q \in Q_0 \cap C^0(\overline{\Omega}) : q|_K \in P_1(K),\ \forall K \in T_{h,0}\}\,.$$

The stress $\boldsymbol{\sigma}$ is approximated in the discontinuous finite element space of piecewise linear functions,

$$\boldsymbol{\Sigma}_{h,0} := \{\boldsymbol{\tau} \in \boldsymbol{\Sigma}_0 : \boldsymbol{\tau}|_K \in P_1(K)^{2\times 2},\ \forall K \in T_{h,0}\}\,.$$

Let $\mathcal{N}_{\widetilde{u}} := dim(\mathbf{U}_{h,0})$ and $\{\overline{\varphi}_i : \overline{\varphi}_i \in \mathbf{U}_{h,0} \text{ for } i \in \mathcal{N}_{\widetilde{u}}\}$ be a set of basis functions for $\mathbf{U}_{h,0}$. Similarly, let $\mathcal{N}_\sigma := dim(\boldsymbol{\Sigma}_{h,0})$ and $\{\overline{\psi}_i : \overline{\psi}_i \in \boldsymbol{\Sigma}_{h,0} \text{ for } i \in \mathcal{N}_\sigma\}$ be a set of basis functions for $\boldsymbol{\Sigma}_{h,0}$. The finite element spaces defined above satisfy the standard approximation properties; see [6] or [22]. It is also well known that the Taylor-Hood pair $(\mathbf{U}_{h,0}, Q_{h,0})$ satisfies the *inf-sup* (or *LBB*) condition,

$$\inf_{0\neq q_h\in Q_{h,0}} \sup_{0\neq \mathbf{v}_h\in \mathbf{U}_{h,0}} \frac{(q_h, \nabla\cdot\mathbf{v}_h)}{\|\mathbf{v}_h\|_1\|q_h\|_0} \ge C\,,$$

where C is a positive constant independent of h.

We consider a discrete mapping $\Psi_{h,t} : \Omega_0 \to \Omega_t$ approximated by P_l Lagrangian finite elements such that $\Psi_{h,t}(y) = \mathbf{x}_h(\mathbf{y}, t)$. The finite element spaces for Ω_t are then defined as

$$\mathbf{U}_{h,t} := \{\mathbf{v}_h : \Omega_t \times [0,T] \to \mathbb{R}^2, \mathbf{v}_h = \overline{\mathbf{v}}_h \circ \Psi_{h,t}^{-1} \text{ for } \overline{\mathbf{v}}_h \in \mathbf{U}_{h,0}\}\,,$$

$$Q_{h,t} := \{q_h : \Omega_t \times [0,T] \to \mathbb{R}, q_h = \overline{q}_h \circ \Psi_{h,t}^{-1} \text{ for } \overline{q}_h \in Q_{h,0}\}\,,$$

$$\boldsymbol{\Sigma}_{h,t} := \{\boldsymbol{\sigma}_h : \Omega_t \times [0,T] \to \mathbb{R}^{2\times 2}, \boldsymbol{\sigma}_h = \overline{\boldsymbol{\sigma}}_h \circ \Psi_t^{-1} \text{ for } \overline{\boldsymbol{\sigma}}_h \in \boldsymbol{\Sigma}_{h,0}\}\,.$$

ETNA
Kent State University
http://etna.math.kent.edu

The approximate solutions $\widetilde{\mathbf{u}}_h$, $\boldsymbol{\sigma}_h$ are expressed as a combination of basis functions multiplied by time-dependent coefficients, i.e.,

$$\widetilde{\mathbf{u}}_h(\mathbf{x},t) = \sum_{i\in\mathcal{N}_{\widetilde{u}}} \widetilde{u}_i(t)\varphi_i(\mathbf{x},t)\,, \qquad \boldsymbol{\sigma}_h(\mathbf{x},t) = \sum_{i\in\mathcal{N}_\sigma} \sigma_i(t)\psi_i(\mathbf{x},t)\,, \tag{3.1}$$

where $\varphi_i := \overline{\varphi}_i \circ \Psi_t^{-1}$ and $\psi_i := \overline{\psi}_i \circ \Psi_t^{-1}$.

For the discrete ALE mapping, define the set

$$\mathbf{X}_h := \{\mathbf{x} \in \mathbf{H}^1(\Omega_0) : \mathbf{x}|_K \in P_l(K)^2,\ \forall K \in T_{h,0}\}\,.$$

If we denote the ith basis function of $\mathbf{X}_h$ by $\hat{\varphi}_i$, then the discrete ALE mapping $\Psi_{h,t}$ provides the discrete coordinate function for $\mathbf{x}$ as

$$\mathbf{x}_h(\mathbf{y},t) = \Psi_{h,t}(\mathbf{y}) = \sum_{i\in\mathcal{N}^{\mathbf{x}}} x_i(t)\hat{\varphi}_i(\mathbf{y})\,,$$

where $\mathcal{N}^{\mathbf{x}}$ is the set of nodal points of $\mathbf{X}_h$. Then the discrete domain velocity $\mathbf{w}_h$ is defined by

$$\mathbf{w}_h(\mathbf{x},t) = \frac{\partial \mathbf{x}_h}{\partial t}\ |_{\mathbf{y}}\ (\Psi_{h,t}^{-1}(\mathbf{x}),t)\,.$$

In order to analyze the convective term $(\widetilde{\mathbf{u}}\cdot\nabla\widetilde{\mathbf{u}},\mathbf{v})_{\Omega_t}$ in the finite element space, we define the trilinear form

$$b(\widetilde{\mathbf{u}},\mathbf{w},\mathbf{v})_{\Omega_t} := \frac{1}{2}\left[(\widetilde{\mathbf{u}}\cdot\nabla\mathbf{w},\mathbf{v})_{\Omega_t} - (\widetilde{\mathbf{u}}\cdot\nabla\mathbf{v},\mathbf{w})_{\Omega_t}\right]\,.$$

Using Green's theorem and $\nabla\cdot\widetilde{\mathbf{u}} = 0$, we obtain

$$(\widetilde{\mathbf{u}}\cdot\nabla\mathbf{w},\mathbf{v})_{\Omega_t} = b(\widetilde{\mathbf{u}},\mathbf{w},\mathbf{v})_{\Omega_t}$$

and

$$b(\widetilde{\mathbf{u}},\mathbf{v},\mathbf{v})_{\Omega_t} = 0 \qquad \forall\mathbf{v}\in\mathbf{U}_{h,t}. \tag{3.2}$$

Since $\nabla\cdot\mathbf{u}^* = 0$, we also have

$$b(\mathbf{u}^*,\mathbf{v},\mathbf{v})_{\Omega_t} = 0 \qquad \forall\mathbf{v}\in\mathbf{U}_{h,t}. \tag{3.3}$$

The following estimate will be used when analyzing the trilinear term [26]:

$$b(\widetilde{\mathbf{u}},\mathbf{w},\mathbf{v})_{\Omega_t} \le C\,\|\widetilde{\mathbf{u}}\|_{1,\Omega_t}\|\mathbf{w}\|_{1,\Omega_t}\|\mathbf{v}\|_{1,\Omega_t}\,. \tag{3.4}$$

We introduce some notation in order to analyze an approximate solution of $\boldsymbol{\sigma}$ by the discontinuous Galerkin method. Define

$$\partial K^-(\mathbf{v}) := \{\mathbf{x}\in\partial K,\ \mathbf{v}\cdot\mathbf{n} < 0\}\,,$$

where ∂K is the boundary of K and $\mathbf{n}$ is the outward unit normal to ∂K,

$$\boldsymbol{\tau}^{\pm}(\mathbf{v}) := \lim_{\epsilon\to 0^{\pm}} \boldsymbol{\tau}(\mathbf{x}+\epsilon\mathbf{v}(\mathbf{x}))\,,$$

ETNA
Kent State University
http://etna.math.kent.edu

and

$$< \boldsymbol{\sigma}^{\pm}, \boldsymbol{\tau}^{\pm} >_{h,\mathbf{v}} := \sum_{K \in T_{h,t}} \int_{\partial K^{-}(\mathbf{v})} (\boldsymbol{\sigma}^{\pm} : \boldsymbol{\tau}^{\pm}) |\mathbf{n} \cdot \mathbf{v}| \, ds \, .$$

Introduce the operator $c(\cdot,\cdot,\cdot)$ defined by

$$c(\mathbf{v}-\mathbf{w}, \boldsymbol{\sigma}, \boldsymbol{\tau})_{\Omega_t} := (((\mathbf{v}-\mathbf{w})\cdot\nabla)\boldsymbol{\sigma}, \boldsymbol{\tau})_{\Omega_t} + \frac{1}{2}(\nabla\cdot\mathbf{v}\,\boldsymbol{\sigma}, \boldsymbol{\tau})_{\Omega_t} + < \boldsymbol{\sigma}^{+} - \boldsymbol{\sigma}^{-}, \boldsymbol{\tau}^{+} >_{h,\mathbf{v}-\mathbf{w}} \, .$$

Note that the second term vanishes when $\nabla \cdot \mathbf{v} = 0$. Using integration by parts and $\widetilde{\mathbf{u}}|_{\Gamma_t} = 0$, we have

$$\begin{aligned} c(\widetilde{\mathbf{u}} - \mathbf{w}, \boldsymbol{\sigma}, \boldsymbol{\tau})_{\Omega_t} = &-(((\widetilde{\mathbf{u}} - \mathbf{w})\cdot\nabla)\boldsymbol{\tau}, \boldsymbol{\sigma})_{\Omega_t} - \frac{1}{2}(\nabla\cdot\widetilde{\mathbf{u}}\,\boldsymbol{\tau}, \boldsymbol{\sigma})_{\Omega_t} \\ &+ < \boldsymbol{\sigma}^{-}, \boldsymbol{\tau}^{-} - \boldsymbol{\tau}^{+} >_{h,\widetilde{\mathbf{u}}-\mathbf{w}} + ((\nabla\cdot\mathbf{w})\boldsymbol{\sigma}, \boldsymbol{\tau})_{\Omega_t} - ((\mathbf{w}\cdot\mathbf{n})\boldsymbol{\sigma}, \boldsymbol{\tau})_{\Gamma_t} \, . \end{aligned}$$

Therefore,

$$\begin{aligned} c(\widetilde{\mathbf{u}}_h - \mathbf{w}_h, \boldsymbol{\sigma}_h, \boldsymbol{\sigma}_h)_{\Omega_t} &= \frac{1}{2}\left[((\nabla\cdot\mathbf{w}_h)\boldsymbol{\sigma}_h, \boldsymbol{\sigma}_h)_{\Omega_t} - ((\mathbf{w}_h\cdot\mathbf{n})\boldsymbol{\sigma}_h, \boldsymbol{\sigma}_h)_{\Omega_t}\right. \\ &\quad \left. + < {\boldsymbol{\sigma}_h}^{+} - {\boldsymbol{\sigma}_h}^{-}, {\boldsymbol{\sigma}_h}^{+} - {\boldsymbol{\sigma}_h}^{-} >_{h,\widetilde{\mathbf{u}}_h-\mathbf{w}_h}\right] \\ &\geq \frac{1}{2}\left[((\nabla\cdot\mathbf{w}_h)\boldsymbol{\sigma}_h, \boldsymbol{\sigma}_h)_{\Omega_t} - ((\mathbf{w}_h\cdot\mathbf{n})\boldsymbol{\sigma}_h, \boldsymbol{\sigma}_h)_{\Gamma_t}\right] \, . \end{aligned} \tag{3.5}$$

Also for $\mathbf{u}^*$ such that $\nabla\cdot\mathbf{u}^* = 0$ and $\mathbf{u}^*|_{\Gamma_t} \neq \mathbf{0}$, we have that

$$c(\mathbf{u}^*, \boldsymbol{\sigma}_h, \boldsymbol{\sigma}_h) \geq \frac{1}{2}((\mathbf{u}^*\cdot\mathbf{n})\boldsymbol{\sigma}_h, \boldsymbol{\sigma}_h)_{\Gamma_t} . \tag{3.6}$$

Consider the semi-discrete variational formulation of the fluid problem in the ALE framework: find $(\widetilde{\mathbf{u}}_h, p_h, \boldsymbol{\sigma}_h)$ such that

$$\begin{aligned} &\lambda\left[\frac{d}{dt}(\boldsymbol{\sigma}_h, \boldsymbol{\tau}_h)_{\Omega_t} + c(\widetilde{\mathbf{u}}_h - \mathbf{w}_h, \boldsymbol{\sigma}_h, \boldsymbol{\tau}_h)_{\Omega_t} + c(\mathbf{u}^*, \boldsymbol{\sigma}_h, \boldsymbol{\tau}_h)_{\Omega_t}\right. \\ &\left. -(\boldsymbol{\sigma}_h(\nabla\cdot\mathbf{w}_h), \boldsymbol{\tau}_h)_{\Omega_t} + (g_a(\boldsymbol{\sigma}_h, \nabla\mathbf{b}),\, \boldsymbol{\tau}_h)_{\Omega_t}\right] + (\boldsymbol{\sigma}_h, \boldsymbol{\tau}_h)_{\Omega_t} - 2\alpha(D(\widetilde{\mathbf{u}}_h), \boldsymbol{\tau}_h)_{\Omega_t} \\ &\qquad = 2\alpha(D(\mathbf{u}^*), \boldsymbol{\tau}_h)_{\Omega_t} \quad \forall \boldsymbol{\tau}_h \in \boldsymbol{\Sigma}_{h,t} \, , \end{aligned} \tag{3.7}$$

$$\begin{aligned} &\rho\left[\frac{d}{dt}(\widetilde{\mathbf{u}}_h, \mathbf{v}_h)_{\Omega_t} + b(\widetilde{\mathbf{u}}_h, \widetilde{\mathbf{u}}_h, \mathbf{v}_h)_{\Omega_t} - (\widetilde{\mathbf{u}}_h(\nabla\cdot\mathbf{w}_h), \mathbf{v}_h)_{\Omega_t} - (\mathbf{w}_h\cdot\nabla\widetilde{\mathbf{u}}_h, \mathbf{v}_h)_{\Omega_t}\right. \\ &\qquad \left. +(\widetilde{\mathbf{u}}_h\cdot\nabla\mathbf{u}^*, \mathbf{v}_h)_{\Omega_t} + (\mathbf{u}^*\cdot\nabla\widetilde{\mathbf{u}}_h, \mathbf{v}_h)_{\Omega_t}\right] \\ &+2(1-\alpha)(D(\widetilde{\mathbf{u}}_h),\, D(\mathbf{v}_h))_{\Omega_t} + (\boldsymbol{\sigma}_h, D(\mathbf{v}_h))_{\Omega_t} + (p_h, \nabla\cdot\mathbf{v}_h)_{\Omega_t} \\ &\qquad = (\mathbf{f}, \mathbf{v}_h)_{\Omega_t} - \rho\left(\frac{\partial\mathbf{u}^*}{\partial t}\,|_{\mathbf{y}} + (\mathbf{u}^* - \mathbf{w})\cdot\nabla\mathbf{u}^*, \mathbf{v}_h\right)_{\Omega_t} \\ &\qquad\quad -2(1-\alpha)(D(\mathbf{u}^*), D(\mathbf{v}_h))_{\Omega_t} \quad \forall \mathbf{v}_h \in \mathbf{U}_{h,t} \, , \end{aligned} \tag{3.8}$$

$$(q_h, \nabla\cdot\widetilde{\mathbf{u}}_h)_{\Omega_t} = 0 \quad \forall q_h \in Q_{h,t} \, . \tag{3.9}$$

ETNA
Kent State University
http://etna.math.kent.edu

Using the bilinear form A_t in (2.15), equations (3.7)–(3.8) are written as

$$\lambda\left[\frac{d}{dt}(\boldsymbol{\sigma}_h,\boldsymbol{\tau}_h)_{\Omega_t}+c(\widetilde{\mathbf{u}}_h-\mathbf{w}_h,\boldsymbol{\sigma}_h,\boldsymbol{\tau}_h)_{\Omega_t}+c(\mathbf{u}^*,\boldsymbol{\sigma}_h,\boldsymbol{\tau}_h)_{\Omega_t}-(\boldsymbol{\sigma}_h(\nabla\cdot\mathbf{w}_h),\boldsymbol{\tau}_h)_{\Omega_t}\right]$$
$$+2\alpha\,\rho\Big[\frac{d}{dt}(\widetilde{\mathbf{u}}_h,\mathbf{v}_h)_{\Omega_t}+b(\widetilde{\mathbf{u}}_h,\widetilde{\mathbf{u}}_h,\mathbf{v}_h)_{\Omega_t}-(\widetilde{\mathbf{u}}_h(\nabla\cdot\mathbf{w}_h),\mathbf{v}_h)_{\Omega_t}-(\mathbf{w}_h\cdot\nabla\widetilde{\mathbf{u}}_h,\mathbf{v}_h)_{\Omega_t}$$
$$+(\widetilde{\mathbf{u}}_h\cdot\nabla\mathbf{u}^*,\mathbf{v}_h)_{\Omega_t}+(\mathbf{u}^*\cdot\nabla\widetilde{\mathbf{u}}_h,\mathbf{v}_h)_{\Omega_t}\Big]+A_t((\boldsymbol{\sigma}_h,\widetilde{\mathbf{u}}_h),(\boldsymbol{\tau}_h,\mathbf{v}_h))$$

$$-2\alpha(p_h,\nabla\cdot\mathbf{v}_h)_{\Omega_t}=(\widetilde{\mathbf{f}},(\mathbf{v}_h,\boldsymbol{\tau}_h))_{\Omega_t}\quad\forall(\mathbf{v}_h,\boldsymbol{\tau}_h)\in\mathbf{U}_h\times\boldsymbol{\Sigma}_h\,, \tag{3.10}$$

where

$$(\widetilde{\mathbf{f}},(\mathbf{v},\boldsymbol{\tau}))_{\Omega_t}:=2\alpha\Big[(\mathbf{f},\mathbf{v})_{\Omega_t}-\rho\left(\frac{\partial\mathbf{u}^*}{\partial t}\,|_{\mathbf{y}}+(\mathbf{u}^*-\mathbf{w})\cdot\nabla\mathbf{u}^*,\mathbf{v}\right)_{\Omega_t}$$
$$-2(1-\alpha)(D(\mathbf{u}^*),D(\mathbf{v}))_{\Omega_t}\Big]+2\alpha\,(D(\mathbf{u}^*),\,\boldsymbol{\tau})_{\Omega_t}\,. \tag{3.11}$$

A conditional energy estimate for the solution of the semi-discrete problem (3.9)–(3.10) is derived in the next theorem.

THEOREM 3.1. *If λM satisfies $1-4\lambda M>0$, a solution to the problem (3.9)–(3.10) satisfies the bound*

$$\alpha\rho\,\|\widetilde{\mathbf{u}}_h\|^2_{0,\Omega_t}+\frac{\lambda}{2}\|\boldsymbol{\sigma}_h\|^2_{0,\Omega_t}+2\alpha(1-\alpha)C_p^2\int_0^t\|D(\widetilde{\mathbf{u}}_h)\|^2_{0,\Omega_t}\,ds$$
$$+\frac{1-4\lambda M}{2}\int_0^t\|\boldsymbol{\sigma}_h\|^2_{0,\Omega_t}\,ds+\frac{\lambda}{2}\int_0^t\int_{\Gamma_t}((\mathbf{u}^*-\mathbf{w}_h)\cdot\mathbf{n})|\boldsymbol{\sigma}_h|^2\,d\Gamma_t\,ds$$
$$\le\alpha\,\rho\,\|\widetilde{\mathbf{u}}_{h,0}\|^2_{0,\Omega_t}+\frac{\lambda}{2}\|\boldsymbol{\sigma}_{h,0}\|^2_{0,\Omega_t}$$
$$+C\int_0^t\left(\|\mathbf{f}\|^2_{-1,\Omega_t}+\left\|\frac{\partial\mathbf{u}^*}{\partial t}\,|_{\mathbf{y}}\right\|^2_{0,\Omega_t}+\|\mathbf{u}^*\|^4_{1,\Omega_t}+\|\mathbf{u}^*\|^2_{1,\Omega_t}\right)\,ds\,, \tag{3.12}$$

where $\widetilde{\mathbf{u}}_{h,0}$, $\boldsymbol{\sigma}_{h,0}$ are interpolants of $\widetilde{\mathbf{u}}_0$ and $\boldsymbol{\sigma}_0$ in $\mathbf{U}_{h,0}$, $\boldsymbol{\Sigma}_{h,0}$, respectively.

Proof. In (3.7)–(3.8) we let $\boldsymbol{\tau}_h=\psi_i$, $\mathbf{v}_h=\varphi_i$, where ψ_i, φ_i are basis functions for $\boldsymbol{\Sigma}_{h,t}$ and $\mathbf{U}_{h,t}$, respectively in (3.1). Unlike a standard fixed domain problem, the choice of $\mathbf{v}_h=\widetilde{\mathbf{u}}_h$ (or $\boldsymbol{\tau}_h=\boldsymbol{\sigma}$) is not generally acceptable because $\widetilde{\mathbf{u}}_h$ and $\mathbf{v}_h$ may have a different time evolution in the time derivative term [32]. If we multiply (3.8) by $\widetilde{u}_i(t)$ and summing over $\mathcal{N}_{\widetilde{u}}$, the time derivative term becomes $\sum_{i\in\mathcal{N}_{\widetilde{u}}}\widetilde{u}_i(t)\frac{d}{dt}(\widetilde{\mathbf{u}}_h,\varphi_i)_{\Omega_t}$ and, using (3.1), $\mathbf{v}_h$ in all other terms can be replaced by $\widetilde{\mathbf{u}}_h$. We obtain from (2.17), (3.1) that

$$\sum_{i\in\mathcal{N}_{\widetilde{u}}}\widetilde{u}_i(t)\frac{d}{dt}(\widetilde{\mathbf{u}}_h,\varphi_i)_{\Omega_t}=\sum_{i\in\mathcal{N}_{\widetilde{u}}}\left[\frac{d}{dt}(\widetilde{\mathbf{u}}_h,\widetilde{u}_i(t)\varphi_i)_{\Omega_t}-(\widetilde{\mathbf{u}}_h,\frac{d\widetilde{u}_i(t)}{dt}\varphi_i)_{\Omega_t}\right]$$
$$=\frac{d}{dt}(\widetilde{\mathbf{u}}_h,\sum_{i\in\mathcal{N}_{\widetilde{u}}}\widetilde{u}_i(t)\varphi_i)_{\Omega_t}-(\widetilde{\mathbf{u}}_h,\sum_{i\in\mathcal{N}_{\widetilde{u}}}\frac{d\widetilde{u}_i(t)}{dt}\varphi_i)_{\Omega_t}$$
$$=\frac{d}{dt}(\widetilde{\mathbf{u}}_h,\widetilde{\mathbf{u}}_h)_{\Omega_t}-(\widetilde{\mathbf{u}}_h,\sum_{i\in\mathcal{N}_{\widetilde{u}}}\frac{\partial(\widetilde{u}_i(t)\varphi_i)}{\partial t}\,|_{\mathbf{y}})_{\Omega_t}$$
$$=\frac{d}{dt}\|\widetilde{\mathbf{u}}_h\|^2_{0,\Omega_t}-(\widetilde{\mathbf{u}}_h,\frac{\partial\widetilde{\mathbf{u}}_h}{\partial t}\,|_{\mathbf{y}})_{\Omega_t}\,.$$

ETNA
Kent State University
http://etna.math.kent.edu

Since $(\widetilde{\mathbf{u}}_h, \frac{\partial \widetilde{\mathbf{u}}_h}{\partial t}\,|_{\mathbf{y}})_{\Omega_t} = \frac{1}{2}(\frac{\partial |\widetilde{\mathbf{u}}_h|^2}{\partial t}\,|_{\mathbf{y}}, 1)_{\Omega_t}$, by (2.18),

$$\sum_{i\in\mathcal{N}_{\widetilde{u}}} \widetilde{u}_i(t)\frac{d}{dt}(\widetilde{\mathbf{u}}_h, \varphi_i)_{\Omega_t} = \frac{d}{dt}\|\widetilde{\mathbf{u}}_h\|^2_{0,\Omega_t} - \frac{1}{2}\frac{d}{dt}\|\widetilde{\mathbf{u}}_h\|^2_{0,\Omega_t} + \frac{1}{2}(\widetilde{\mathbf{u}}_h(\nabla\cdot\mathbf{w}_h), \widetilde{\mathbf{u}}_h)_{\Omega_t}$$
$$= \frac{1}{2}\frac{d}{dt}\|\widetilde{\mathbf{u}}_h\|^2_{0,\Omega_t} + \frac{1}{2}(\widetilde{\mathbf{u}}_h(\nabla\cdot\mathbf{w}_h), \widetilde{\mathbf{u}}_h)_{\Omega_t}\,. \tag{3.13}$$

By the same argument, we get

$$\sum_{i\in\mathcal{N}_\sigma} \sigma_i(t)\frac{d}{dt}(\boldsymbol{\sigma}_h, \psi_i)_{\Omega_t} = \frac{1}{2}\frac{d}{dt}\|\boldsymbol{\sigma}_h\|^2_{0,\Omega_t} + \frac{1}{2}(\boldsymbol{\sigma}_h(\nabla\cdot\mathbf{w}_h), \boldsymbol{\sigma}_h)_{\Omega_t}\,. \tag{3.14}$$

Therefore, using (2.11), (2.16), (3.2), (3.3), (3.5), (3.6), (3.9), (3.13), and (3.14), equation (3.10) implies that

$$\lambda\left[\frac{1}{2}\frac{d}{dt}\|\boldsymbol{\sigma}_h\|^2_{0,\Omega_t} + \frac{1}{2}(((\mathbf{u}^* - \mathbf{w}_h)\cdot\mathbf{n})\boldsymbol{\sigma}_h, \boldsymbol{\sigma}_h)_{\Gamma_t}\right] \tag{3.15}$$
$$+ 2\alpha\,\rho\left(\frac{1}{2}\frac{d}{dt}\|\widetilde{\mathbf{u}}_h\|^2_{0,\Omega_t} - \frac{1}{2}(\widetilde{\mathbf{u}}_h(\nabla\cdot\mathbf{w}_h)), \widetilde{\mathbf{u}}_h)_{\Omega_t} - (\mathbf{w}_h\cdot\nabla\widetilde{\mathbf{u}}_h, \widetilde{\mathbf{u}}_h)_{\Omega_t} - \epsilon\|\widetilde{\mathbf{u}}_h\|^2_{1,\Omega_t}\right)$$
$$+ (1 - 4\lambda M)\|\boldsymbol{\sigma}_h\|^2_{0,\Omega_t} + 4\alpha(1-\alpha)C_p^2\|\widetilde{\mathbf{u}}\|^2_{1,\Omega_t} \le (\widetilde{\mathbf{f}}, (\widetilde{\mathbf{u}}_h, \boldsymbol{\sigma}_h))_{\Omega_t}\,.$$

By the Cauchy-Schwarz inequality, Young's inequality, (2.10) and (3.4),

$$(\widetilde{\mathbf{f}}, (\widetilde{\mathbf{u}}_h, \boldsymbol{\sigma}_h))_{\Omega_t} \le C\left[\|\mathbf{f}\|^2_{-1,\Omega_t} + \left\|\frac{\partial \mathbf{u}^*}{\partial t}\right\|^2_{0,\Omega_t} + \|\mathbf{u}^*\|^4_{1,\Omega_t} + \|\mathbf{u}^*\|^2_{1,\Omega_t}\right] \tag{3.16}$$
$$+\delta_1\|\widetilde{\mathbf{u}}_h\|^2_{1,\Omega_t} + \delta_2\|\boldsymbol{\sigma}_h\|^2_{0,\Omega_t}.$$

for arbitrary $\delta_1,\ \delta_2 > 0$. Now the estimates (3.15), (3.16) and the identity

$$(\mathbf{w}_h\cdot\nabla\widetilde{\mathbf{u}}_h, \widetilde{\mathbf{u}}_h)_{\Omega_t} = -\frac{1}{2}((\nabla\cdot\mathbf{w}_h))\widetilde{\mathbf{u}}_h, \widetilde{\mathbf{u}}_h)_{\Omega_t}\,,$$

imply that

$$\alpha\rho\frac{d}{dt}\|\widetilde{\mathbf{u}}_h\|^2_{0,\Omega_t} + \frac{\lambda}{2}\frac{d}{dt}\|\boldsymbol{\sigma}_h\|^2_{0,\Omega_t} + (4\alpha(1-\alpha)C_p^2 - 2\alpha\,\rho\epsilon - \delta_1)\|D(\widetilde{\mathbf{u}}_h)\|^2_{0,\Omega_t}$$
$$+ (1 - 4\lambda M - \delta_2)\|\boldsymbol{\sigma}_h\|^2_{0,\Omega_t} + \frac{\lambda}{2}(((\mathbf{u}^* - \mathbf{w}_h)\cdot\mathbf{n})\boldsymbol{\sigma}_h, \boldsymbol{\sigma}_h)_{\Gamma_t}$$
$$\le C\left[\|\mathbf{f}\|^2_{-1,\Omega_t} + \left\|\frac{\partial \mathbf{u}^*}{\partial t}\right\|^2_{0,\Omega_t} + \|\mathbf{u}^*\|^4_{1,\Omega_t} + \|\mathbf{u}^*\|^2_{1,\Omega_t}\right]\,.$$

The bound (3.12) follows by letting $\epsilon = \frac{2\alpha(1-\alpha)C_p^2}{2\alpha\rho+1}$, $\delta_1 = \epsilon$, $\delta_2 = \frac{1-4\lambda M}{2}$ and integrating over $(0,t)$. ∎

REMARK 3.2. Note that the boundary integral in (3.12),

$$\int_{\Gamma_t} ((\mathbf{u}^* - \mathbf{w}_h)\cdot\mathbf{n})|\boldsymbol{\sigma}_h|^2\, d\Gamma_t,$$

is nonnegative if $(\mathbf{u}^* - \mathbf{w}_h)\cdot\mathbf{n} \ge 0$. Since $\mathbf{u}^* - \mathbf{w}_h$ represents the relative velocity of the fluid, under the assumption of a homogeneous stress condition on the inflow boundary, where $(\mathbf{u}^* - \mathbf{w}_h)\cdot\mathbf{n} < 0$, this term may be deleted. Therefore, an unconditional stability estimate can be obtained. This is also the case for the stability estimate, (4.6) below, of the fully discretized problem by a first-order scheme.

ETNA
Kent State University
http://etna.math.kent.edu

4. Time discretization. In the implemention of the ALE method there is a condition on the time integration scheme, referred to as the *geometric conservation law* (GCL), which is considered to be related to the consistency of numerical solutions [5, 15, 16, 32]. The GCL requires a numerical time discretization scheme to simulate a uniform flow exactly on a moving domain. The GCL in the finite element ALE framework suggests that a quadrature rule should be chosen so that the time integration

$$\int_{\Omega_{t^{n+1}}} \mathbf{v}_h \, d\Omega - \int_{\Omega_{t^n}} \mathbf{v}_h \, d\Omega = \int_{t^n}^{t^{n+1}} \int_{\Omega_t} \mathbf{v}_h \nabla \cdot \mathbf{w}_h \, d\Omega \, dt \approx \int_{t^n}^{t^{n+1}} \mathbf{p}(s) \, ds \tag{4.1}$$

is performed exactly, where $\mathbf{p}(t)$ is a polynomial for $t \in [t^n, t^{n+1}]$ of degree $k \times d - 1$, where d is the dimension [35]. For example, a quadrature formula with the degree of precision 1 or higher satisfies the GCL if $d = 2$ and piecewise linear elements are used for the ALE mapping Ψ_t. Thus, the mid-point rule or the trapezoidal rule satisfies (4.1).

It was reported in [23] that when a temporal discretization not satisfying the GCL is applied to a moving mesh problem, its accuracy may not be as high as the scheme on a fixed domain. The authors also pointed out that a higher-order method not satisfying the GCL tends to lose more accuracy than a lower-order method. However, the effect of the GCL on stability was not clearly verified analytically and numerically. Some other studies on the GCL condition applied to the ALE finite element formulation also can be found in [5, 16].

We will investigate the stability of fully discretized systems by first-order and second-order methods, respectively. Throughout this section we use $\mathbf{u}^n$ to denote $\mathbf{u}_h^n$, an approximation of $\mathbf{u}_h(t^n)$, to simplify our notation. The standard first-order method is given below.

ALGORITHM 4.1 (First-order non-GCL). *Find* $(\boldsymbol{\sigma}^{n+1}, \widetilde{\mathbf{u}}^{n+1}, p^{n+1})$ *satisfying*

$$\begin{aligned}
&\lambda \left[(\boldsymbol{\sigma}^{n+1}, \boldsymbol{\tau})_{\Omega_{t_{n+1}}} - (\boldsymbol{\sigma}^n, \boldsymbol{\tau})_{\Omega_{t_n}} \right] + \lambda \, \Delta t \left[c(\widetilde{\mathbf{u}}^{n+1} - \mathbf{w}^{n+1}, \boldsymbol{\sigma}^{n+1}, \boldsymbol{\tau})_{\Omega_{t^{n+1}}} \right. \\
&\qquad + c(\mathbf{u}^{*n+1}, \boldsymbol{\sigma}^{n+1}, \boldsymbol{\tau})_{\Omega_{t^{n+1}}} - (\boldsymbol{\sigma}^{n+1}(\nabla \cdot \mathbf{w}^{n+1}), \boldsymbol{\tau})_{\Omega_{t^{n+1}}} \\
&\qquad \left. + (g_a(\boldsymbol{\sigma}^{n+1}, \nabla \mathbf{b}^{n+1}), \, \boldsymbol{\tau})_{\Omega_{t^{n+1}}} \right] \\
&\qquad + \Delta t \left[(\boldsymbol{\sigma}^{n+1}, \boldsymbol{\tau})_{\Omega_{t^{n+1}}} - 2\alpha (D(\widetilde{\mathbf{u}}^{n+1}), \boldsymbol{\tau})_{\Omega_{t^{n+1}}} \right] \\
&\qquad\qquad = 2\alpha \, \Delta t (D(\mathbf{u}^{*n+1}), \boldsymbol{\tau})_{\Omega_{t^{n+1}}} \ \forall \boldsymbol{\tau} \in \boldsymbol{\Sigma}_{h,t} \, ,
\end{aligned}$$

$$\begin{aligned}
&\rho \left[(\widetilde{\mathbf{u}}^{n+1}, \mathbf{v})_{\Omega_{t^{n+1}}} - (\widetilde{\mathbf{u}}^n, \mathbf{v})_{\Omega_{t_n}} \right] + \Delta t \, \rho \left[b(\widetilde{\mathbf{u}}^{n+1}, \widetilde{\mathbf{u}}^{n+1}, \mathbf{v})_{\Omega_{t^{n+1}}} \right. \\
&\qquad - (\widetilde{\mathbf{u}}^{n+1}(\nabla \cdot \mathbf{w}^{n+1}), \mathbf{v})_{\Omega_{t^{n+1}}} - (\mathbf{w}^{n+1} \cdot \nabla \widetilde{\mathbf{u}}^{n+1}, \mathbf{v})_{\Omega_{t^{n+1}}} \\
&\qquad \left. + (\widetilde{\mathbf{u}}^{n+1} \cdot \nabla \mathbf{u}^{*n+1}, \mathbf{v})_{\Omega_{t^{n+1}}} + (\mathbf{u}^{*n+1} \cdot \nabla \widetilde{\mathbf{u}}^{n+1}, \mathbf{v})_{\Omega_{t^{n+1}}} \right] \\
&\qquad + \Delta t \left[2(1-\alpha)(D(\widetilde{\mathbf{u}}^{n+1}), \, D(\mathbf{v}))_{\Omega_{t^{n+1}}} + (\boldsymbol{\sigma}^{n+1}, D(\mathbf{v}))_{\Omega_{t^{n+1}}} \right. \\
&\qquad \left. + (p^{n+1}, \nabla \cdot \mathbf{v})_{\Omega_{t^{n+1}}} \right] \\
&\qquad = \Delta t \left[(\mathbf{f}^{n+1}, \mathbf{v})_{\Omega_{t^{n+1}}} - \right. \\
&\qquad\qquad \rho \left(\frac{\partial \mathbf{u}^{*\,n+1}}{\partial t} \Big|_{\mathbf{y}} + (\mathbf{u}^{*n+1} - \mathbf{w}^{n+1}) \cdot \nabla \mathbf{u}^{*n+1}, \mathbf{v} \right)_{\Omega_{t^{n+1}}} \\
&\qquad\qquad \left. - 2(1-\alpha)(D(\mathbf{u}^{*n+1}), D(\mathbf{v}))_{\Omega_{t^{n+1}}} \right] \ \forall \mathbf{v} \in \mathbf{U}_{h,t} \, ,
\end{aligned}$$

$$(q, \nabla \cdot \widetilde{\mathbf{u}}^{n+1})_{\Omega_{t^{n+1}}} = 0 \quad \forall q \in Q_{h,t} \, .$$

ETNA
Kent State University
http://etna.math.kent.edu

The above scheme, however, does not satisfy (4.1). If we apply the mid-point rule

$$\int_{\Omega_{t^{n+1}}} \mathbf{v}_h \, d\Omega - \int_{\Omega_{t^n}} \mathbf{v}_h \, d\Omega = \int_{t^n}^{t^{n+1}} \int_{\Omega_t} \mathbf{v}_h \nabla \cdot \mathbf{w}_h \, d\Omega \, dt \approx \Delta t \int_{\Omega_{t^{n+\frac{1}{2}}}} \mathbf{v}_h \nabla \cdot \mathbf{w}_h \, ds \tag{4.2}$$

for time integration, the first-order scheme is given below.

ALGORITHM 4.2 (First-order GCL). *Find* $(\boldsymbol{\sigma}^{n+1}, \widetilde{\mathbf{u}}^{n+1}, p^{n+1})$ *satisfying*

$$\begin{aligned}
&\lambda \left[(\boldsymbol{\sigma}^{n+1}, \boldsymbol{\tau})_{\Omega_{t_{n+1}}} - (\boldsymbol{\sigma}^n, \boldsymbol{\tau})_{\Omega_{t_n}} \right] \\
&+\lambda \, \Delta t \left[c(\widetilde{\mathbf{u}}^{n+1} - \mathbf{w}^{n+\frac{1}{2}}, \boldsymbol{\sigma}^{n+1}, \boldsymbol{\tau})_{\Omega_{t^{n+\frac{1}{2}}}} + c(\mathbf{u}^{*n+1}, \boldsymbol{\sigma}^{n+1}, \boldsymbol{\tau})_{\Omega_{t^{n+\frac{1}{2}}}} \right. \\
&\qquad \left. -(\boldsymbol{\sigma}^{n+1}(\nabla \cdot \mathbf{w}^{n+\frac{1}{2}}), \boldsymbol{\tau})_{\Omega_{t^{n+\frac{1}{2}}}} + (g_a(\boldsymbol{\sigma}^{n+1}, \nabla \mathbf{b}^{n+1}), \, \boldsymbol{\tau})_{\Omega_{t^{n+\frac{1}{2}}}} \right] \\
&+\Delta t \left[(\boldsymbol{\sigma}^{n+1}, \boldsymbol{\tau})_{\Omega_{t^{n+\frac{1}{2}}}} - 2\alpha (D(\widetilde{\mathbf{u}}^{n+1}), \boldsymbol{\tau})_{\Omega_{t^{n+\frac{1}{2}}}} \right] \\
&= 2\alpha \, \Delta t (D(\mathbf{u}^{*n+1}), \boldsymbol{\tau})_{\Omega_{t^{n+\frac{1}{2}}}} ,
\end{aligned} \tag{4.3}$$

$$\begin{aligned}
&\rho \left[(\widetilde{\mathbf{u}}^{n+1}, \mathbf{v})_{\Omega_{t^{n+1}}} - (\widetilde{\mathbf{u}}^n, \mathbf{v})_{\Omega_{t_n}} \right] + \Delta t \, \rho \left[b(\widetilde{\mathbf{u}}^{n+1}, \widetilde{\mathbf{u}}^{n+1}, \mathbf{v})_{\Omega_{t^{n+\frac{1}{2}}}} \right. \\
&\qquad -(\widetilde{\mathbf{u}}^{n+1}(\nabla \cdot \mathbf{w}^{n+\frac{1}{2}}), \mathbf{v})_{\Omega_{t^{n+\frac{1}{2}}}} - (\mathbf{w}^{n+\frac{1}{2}} \cdot \nabla \widetilde{\mathbf{u}}^{n+1}, \mathbf{v})_{\Omega_{t^{n+\frac{1}{2}}}} \\
&\qquad \left. +(\widetilde{\mathbf{u}}^{n+1} \cdot \nabla \mathbf{u}^{*n+1}, \mathbf{v})_{\Omega_{t^{n+\frac{1}{2}}}} + (\mathbf{u}^{*n+1} \cdot \nabla \widetilde{\mathbf{u}}^{n+1}, \mathbf{v})_{\Omega_{t^{n+\frac{1}{2}}}} \right] \\
&\qquad +\Delta t \big[2(1-\alpha)(D(\widetilde{\mathbf{u}}^{n+1}), \, D(\mathbf{v}))_{\Omega_{t^{n+\frac{1}{2}}}} + (\boldsymbol{\sigma}^{n+1}, D(\mathbf{v}))_{\Omega_{t^{n+\frac{1}{2}}}} \\
&\qquad\quad +(p^{n+1}, \nabla \cdot \mathbf{v})_{\Omega_{t^{n+\frac{1}{2}}}} \big] \\
&\qquad = \Delta t \left[(\mathbf{f}^{n+\frac{1}{2}}, \mathbf{v})_{\Omega_{t^{n+\frac{1}{2}}}} \right. \\
&\qquad\quad -\rho \left(\frac{\partial \mathbf{u}^{*\,n+1}}{\partial t} |_{\mathbf{y}} + (\mathbf{u}^{*n+1} - \mathbf{w}^{n+\frac{1}{2}}) \cdot \nabla \mathbf{u}^{*n+1}, \mathbf{v} \right)_{\Omega_{t^{n+\frac{1}{2}}}} \\
&\qquad\quad \left. -2(1-\alpha)(D(\mathbf{u}^{*n+1}), D(\mathbf{v}))_{\Omega_{t^{n+\frac{1}{2}}}} \right] ,
\end{aligned} \tag{4.4}$$

$$(q, \nabla \cdot \widetilde{\mathbf{u}}^{n+1})_{\Omega_{t^{n+\frac{1}{2}}}} = 0 \, , \tag{4.5}$$

for all $(\boldsymbol{\tau}, \mathbf{v}, q) \in \boldsymbol{\Sigma}_{h,t} \times \mathbf{U}_{h,t} \times Q_{h,t}$.

ETNA
Kent State University
http://etna.math.kent.edu

THEOREM 4.3. *A solution to the fully discretized system (4.3)–(4.5) satisfies the inequality*

$$
\begin{aligned}
(4.6)\qquad & \frac{\lambda}{2}\|\boldsymbol{\sigma}^{n+1}\|^2_{0,\Omega_{t^{n+1}}} + \alpha\rho\|\widetilde{\mathbf{u}}^{n+1}\|^2_{1,\Omega_{t^{n+1}}} \\
&\qquad +\Delta t\sum_{i=0}^{n}\left[2\alpha(1-\alpha)C_p^2\|\widetilde{\mathbf{u}}^{i+1}\|^2_{1,\Omega_{t^{i+\frac12}}} + \frac{1-4\lambda M}{2}\|\boldsymbol{\sigma}^{i+1}\|^2_{0,\Omega_{t^{i+\frac12}}}\right] \\
&\qquad +\Delta t\,\frac{\lambda}{2}\sum_{i=0}^{n}\int_{\Gamma_{t^{i+\frac12}}}((\mathbf{u}^{*i+1}-\mathbf{w}^{i+1})\cdot\mathbf{n})|\boldsymbol{\sigma}^{i+1}|^2\,d\Gamma_{t^{i+\frac12}} \\
&\le \frac{\lambda}{2}\|\boldsymbol{\sigma}^{0}\|^2_{0,\Omega_0} + \alpha\rho\|\widetilde{\mathbf{u}}^{0}\|^2_{1,\Omega_0} \\
&\qquad +C\,\Delta t\sum_{i=0}^{n}\left[\|\mathbf{f}^{i+\frac12}\|^2_{-1,\Omega_{t^{i+\frac12}}} + \left\|\frac{\partial\mathbf{u}^{*\,i+1}}{\partial t}\right|_{\mathbf{y}}\right\|^2_{0,\Omega_{t^{i+\frac12}}} \right. \\
&\qquad\qquad \left. +\|\mathbf{u}^{*i+1}\|^4_{1,\Omega_{t^{i+\frac12}}} + \|\mathbf{u}^{*i+1}\|^2_{1,\Omega_{t^{i+\frac12}}}\right].
\end{aligned}
$$

Proof. Letting $\boldsymbol{\tau}=\boldsymbol{\sigma}^{n+1}$, $\mathbf{v}=\widetilde{\mathbf{u}}^{n+1}$ and $q=p^{n+1}$ in (4.3)–(4.5), we obtain

$$
\begin{aligned}
(4.7)\quad & \lambda\|\boldsymbol{\sigma}^{n+1}\|^2_{0,\Omega_{t^{n+1}}} + 2\alpha\,\rho\|\widetilde{\mathbf{u}}^{n+1}\|^2_{1,\Omega_{t^{n+1}}} \\
&\quad +\lambda\,\Delta t\left[c(\widetilde{\mathbf{u}}^{n+1}-\mathbf{w}^{n+\frac12},\boldsymbol{\sigma}^{n+1},\boldsymbol{\sigma}^{n+1})_{\Omega_{t^{n+\frac12}}}\right. \\
&\quad \left. +c(\mathbf{u}^{*n+1},\boldsymbol{\sigma}^{n+1},\boldsymbol{\sigma}^{n+1})_{\Omega_{t^{n+\frac12}}} - (\boldsymbol{\sigma}^{n+1}(\nabla\cdot\mathbf{w}^{n+\frac12}),\boldsymbol{\sigma}^{n+1})_{\Omega_{t^{n+\frac12}}}\right] \\
&\quad +2\Delta t\,\alpha\rho\left[b(\widetilde{\mathbf{u}}^{n+1},\widetilde{\mathbf{u}}^{n+1},\widetilde{\mathbf{u}}^{n+1})_{\Omega_{t^{n+\frac12}}} - (\widetilde{\mathbf{u}}^{n+1}(\nabla\cdot\mathbf{w}^{n+\frac12}),\widetilde{\mathbf{u}}^{n+1})_{\Omega_{t^{n+\frac12}}}\right. \\
&\quad -(\mathbf{w}^{n+\frac12}\cdot\nabla\widetilde{\mathbf{u}}^{n+1},\widetilde{\mathbf{u}}^{n+1})_{\Omega_{t^{n+\frac12}}} + (\widetilde{\mathbf{u}}^{n+1}\cdot\nabla\mathbf{u}^{*n+1},\widetilde{\mathbf{u}}^{n+1})_{\Omega_{t^{n+\frac12}}} \\
&\quad \left. +(\mathbf{u}^{*n+1}\cdot\nabla\widetilde{\mathbf{u}}^{n+1},\widetilde{\mathbf{u}}^{n+1})_{\Omega_{t^{n+\frac12}}}\right] \\
&\quad +\Delta t\,A_t((\boldsymbol{\sigma}^{n+1},\widetilde{\mathbf{u}}^{n+1}),(\boldsymbol{\sigma}^{n+1},\widetilde{\mathbf{u}}^{n+1}))_{\Omega_{t^{n+\frac12}}} \\
&= \lambda(\boldsymbol{\sigma}^{n},\boldsymbol{\sigma}^{n+1})_{\Omega_{t_n}} + 2\alpha\,\rho(\widetilde{\mathbf{u}}^{n},\widetilde{\mathbf{u}}^{n+1})_{\Omega_{t^n}} + \Delta t\,(\widetilde{\mathbf{f}}^{n+\frac12},(\mathbf{u}^{n+1},\boldsymbol{\sigma}^{n+1}))_{\Omega_{t^{n+\frac12}}},
\end{aligned}
$$

where $(\widetilde{\mathbf{f}}^{n+\frac12},(\mathbf{u}^{n+1},\boldsymbol{\sigma}^{n+1}))_{\Omega_{t^{n+\frac12}}}$ is defined as (3.11). By (2.11), (3.2), (3.5), (3.6), we have

$$
\begin{aligned}
(4.8)\qquad & c(\widetilde{\mathbf{u}}^{n+1}-\mathbf{w}^{n+\frac12},\boldsymbol{\sigma}^{n+1},\boldsymbol{\sigma}^{n+1})_{\Omega_{t^{n+\frac12}}} + c(\mathbf{u}^{*n+1},\boldsymbol{\sigma}^{n+1},\boldsymbol{\sigma}^{n+1})_{\Omega_{t^{n+\frac12}}} \\
&\qquad -(\boldsymbol{\sigma}^{n+1}(\nabla\cdot\mathbf{w}^{n+\frac12}),\boldsymbol{\sigma}^{n+1})_{\Omega_{t^{n+\frac12}}} \\
&\ge -\frac{1}{2}(\boldsymbol{\sigma}^{n+1}(\nabla\cdot\mathbf{w}^{n+\frac12}),\boldsymbol{\sigma}^{n+1})_{\Omega_{t^{n+\frac12}}} \\
&\qquad +\frac{1}{2}(((\mathbf{u}^{*n+1}-\mathbf{w}^{n+\frac12})\cdot\mathbf{n})\boldsymbol{\sigma}^{n+1},\boldsymbol{\sigma}^{n+1})_{\Gamma_{t^{n+\frac12}}},
\end{aligned}
$$

ETNA
Kent State University
http://etna.math.kent.edu

and

$$
\begin{aligned}
(4.9)\quad & b(\widetilde{\mathbf{u}}^{n+1},\widetilde{\mathbf{u}}^{n+1},\widetilde{\mathbf{u}}^{n+1})_{\Omega_{t^{n+\frac12}}} - (\widetilde{\mathbf{u}}^{n+1}(\nabla\cdot\mathbf{w}^{n+\frac12}),\widetilde{\mathbf{u}}^{n+1})_{\Omega_{t^{n+\frac12}}} \\
& - (\mathbf{w}^{n+\frac12}\cdot\nabla\widetilde{\mathbf{u}}^{n+1},\widetilde{\mathbf{u}}^{n+1})_{\Omega_{t^{n+\frac12}}} + (\widetilde{\mathbf{u}}^{n+1}\cdot\nabla\mathbf{u}^{*n+1},\widetilde{\mathbf{u}}^{n+1})_{\Omega_{t^{n+\frac12}}} \\
& + (\mathbf{u}^{*n+1}\cdot\nabla\widetilde{\mathbf{u}}^{n+1},\widetilde{\mathbf{u}}^{n+1})_{\Omega_{t^{n+\frac12}}} \\
& \geq -\frac{1}{2}(\widetilde{\mathbf{u}}^{n+1}(\nabla\cdot\mathbf{w}^{n+\frac12}),\widetilde{\mathbf{u}}^{n+1})_{\Omega_{t^{n+\frac12}}} - \epsilon\|\widetilde{\mathbf{u}}^{n+1}\|_{1,\Omega_{t^{n+\frac12}}}.
\end{aligned}
$$

Therefore, using (2.16), (4.2), (4.8) and (4.9), we obtain a lower bound for the left hand side of (4.7):

$$
\begin{aligned}
(4.10)\quad \text{LHS} \geq\ & \frac{\lambda}{2}\left[\|\boldsymbol{\sigma}^{n+1}\|^2_{0,\Omega_{t^{n+1}}} + \|\boldsymbol{\sigma}^{n+1}\|^2_{0,\Omega_{t^n}}\right] \\
& + \alpha\rho\left[\|\widetilde{\mathbf{u}}^{n+1}\|^2_{1,\Omega_{t^{n+1}}} - \|\widetilde{\mathbf{u}}^{n+1}\|^2_{1,\Omega_{t^n}}\right] \\
& + \Delta t\left[(1-4\lambda M)\|\boldsymbol{\sigma}^{n+1}\|^2_{0,\Omega_{t^{n+\frac12}}} + (4\alpha(1-\alpha)C_p^2 - 2\alpha\rho\epsilon)\|\widetilde{\mathbf{u}}^{n+1}\|^2_{1,\Omega_{t^{n+\frac12}}}\right] \\
& + \Delta t\,\frac{\lambda}{2}(((\mathbf{u}^{*n+1}-\mathbf{w}^{n+1})\cdot\mathbf{n})\boldsymbol{\sigma}^{n+1},\boldsymbol{\sigma}^{n+1})_{\Gamma_{t^{n+\frac12}}}.
\end{aligned}
$$

On the other hand, we have an upper bound for the right side of (4.7) by (2.10), (3.4), the Poincaré inequality and Young's inequality:

$$
\begin{aligned}
(4.11)\quad \text{RHS} \leq\ & \frac{\lambda}{2}\|\boldsymbol{\sigma}^n\|^2_{0,\Omega_{t^n}} + \frac{\lambda}{2}\|\boldsymbol{\sigma}^{n+1}\|^2_{0,\Omega_{t^n}} + \alpha\rho\|\widetilde{\mathbf{u}}^n\|^2_{1,\Omega_{t^n}} + \alpha\rho\|\widetilde{\mathbf{u}}^{n+1}\|^2_{1,\Omega_{t^n}} \\
& + C\,\Delta t\left[\|\mathbf{f}^{n+\frac12}\|^2_{-1,\Omega_{t^{n+\frac12}}} + \left\|\frac{\partial\mathbf{u}^{*\,n+1}}{\partial t}\,|_{\mathbf{y}}\right\|^2_{0,\Omega_{t^{n+\frac12}}}\right. \\
& \left. + \|\mathbf{u}^{*n+1}\|^4_{1,\Omega_{t^{n+\frac12}}} + \|\mathbf{u}^{*n+1}\|^2_{1,\Omega_{t^{n+\frac12}}}\right] \\
& + \delta_1\|\widetilde{\mathbf{u}}^{n+1}\|^2_{1,\Omega_{t^{n+\frac12}}} + \delta_2\|\boldsymbol{\sigma}^{n+1}\|^2_{0,\Omega_{t^{n+\frac12}}}
\end{aligned}
$$

for $\delta_1,\ \delta_2 > 0$. Choosing $\epsilon = \frac{2\alpha(1-\alpha)C_p^2}{2\alpha\rho+1}$, $\delta_1 = \epsilon$, $\delta_2 = \frac{1-4\lambda M}{2}$, we get from (4.10)–(4.11) that

$$
\begin{aligned}
(4.12)\quad & \frac{\lambda}{2}\|\boldsymbol{\sigma}^{n+1}\|^2_{0,\Omega_{t^{n+1}}} + \alpha\rho\|\widetilde{\mathbf{u}}^{n+1}\|^2_{1,\Omega_{t^{n+1}}} \\
& + \Delta t\left[2\alpha(1-\alpha)C_p^2\|\widetilde{\mathbf{u}}^{n+1}\|^2_{1,\Omega_{t^{n+\frac12}}} + \frac{1-4\lambda M}{2}\|\boldsymbol{\sigma}^{n+1}\|^2_{0,\Omega_{t^{n+\frac12}}}\right] \\
& + \Delta t\,\frac{\lambda}{2}(((\mathbf{u}^{*n+1}-\mathbf{w}^{n+1})\cdot\mathbf{n})\boldsymbol{\sigma}^{n+1},\boldsymbol{\sigma}^{n+1})_{\Gamma_{t^{n+\frac12}}} \\
\leq\ & \frac{\lambda}{2}\|\boldsymbol{\sigma}^n\|^2_{\Omega_{t^n}} + \alpha\rho\|\widetilde{\mathbf{u}}^n\|^2_{\Omega_{t^n}} + C\,\Delta t\left[\|\mathbf{f}^{n+\frac12}\|^2_{-1,\Omega_{t^{n+\frac12}}} + \left\|\frac{\partial\mathbf{u}^{*\,n+1}}{\partial t}\right\|^2_{0,\Omega_{t^{n+\frac12}}}\right. \\
& \left. + \|\mathbf{u}^{*n+1}\|^4_{1,\Omega_{t^{n+\frac12}}} + \|\mathbf{u}^{*n+1}\|^2_{1,\Omega_{t^{n+\frac12}}}\right].
\end{aligned}
$$

ETNA
Kent State University
http://etna.math.kent.edu

Summing over all times steps in (4.12), we obtain (4.6). □

Next, we consider the second order scheme based on (4.2).

ALGORITHM 4.4 (Second-order GCL). *Find* $(\boldsymbol{\sigma}^{n+1}, \widetilde{\mathbf{u}}^{n+1}, p^{n+1})$ *satisfying*

$$
\begin{aligned}
(4.13)\ & \lambda \left[(\boldsymbol{\sigma}^{n+1}, \boldsymbol{\tau})_{\Omega_{t_{n+1}}} - (\boldsymbol{\sigma}^{n}, \boldsymbol{\tau})_{\Omega_{t_n}} \right] \\
& + \lambda\, \Delta t \Bigg[c\left(\frac{\widetilde{\mathbf{u}}^{n+1} + \widetilde{\mathbf{u}}^{n}}{2} - \mathbf{w}^{n+\frac{1}{2}}, \frac{\boldsymbol{\sigma}^{n+1} + \boldsymbol{\sigma}^{n}}{2}, \boldsymbol{\tau} \right)_{\Omega_{t^{n+\frac{1}{2}}}} \\
& + c\left(\mathbf{u}^{*n+\frac{1}{2}}, \frac{\boldsymbol{\sigma}^{n+1} + \boldsymbol{\sigma}^{n}}{2}, \boldsymbol{\tau} \right)_{\Omega_{t^{n+\frac{1}{2}}}} - \left(\frac{\boldsymbol{\sigma}^{n+1} + \boldsymbol{\sigma}^{n}}{2} (\nabla \cdot \mathbf{w}^{n+\frac{1}{2}}), \boldsymbol{\tau} \right)_{\Omega_{t^{n+\frac{1}{2}}}} \\
& \qquad + \left(g_a \left(\frac{\boldsymbol{\sigma}^{n+1} + \boldsymbol{\sigma}^{n}}{2}, \nabla \mathbf{b}^{n+\frac{1}{2}} \right), \boldsymbol{\tau} \right)_{\Omega_{t^{n+\frac{1}{2}}}} \Bigg] \\
& + \Delta t \left[\left(\frac{\boldsymbol{\sigma}^{n+1} + \boldsymbol{\sigma}^{n}}{2}, \boldsymbol{\tau} \right)_{\Omega_{t^{n+\frac{1}{2}}}} - 2\alpha \left(D\left(\frac{\widetilde{\mathbf{u}}^{n+1} + \widetilde{\mathbf{u}}^{n}}{2} \right), \boldsymbol{\tau} \right)_{\Omega_{t^{n+\frac{1}{2}}}} \right] \\
& \qquad = 2\alpha\, \Delta t (D(\mathbf{u}^{*n+\frac{1}{2}}), \boldsymbol{\tau})_{\Omega_{t^{n+\frac{1}{2}}}} \quad \forall \boldsymbol{\tau} \in \boldsymbol{\Sigma}_{h,t}\,,
\end{aligned}
$$

$$
\begin{aligned}
(4.14)\ & \rho \left[(\widetilde{\mathbf{u}}^{n+1}, \mathbf{v})_{\Omega_{t^{n+1}}} - (\widetilde{\mathbf{u}}_h, \mathbf{v})_{\Omega_{t_n}} \right] \\
& + \Delta t\, \rho \Bigg[b\left(\frac{\widetilde{\mathbf{u}}^{n+1} + \widetilde{\mathbf{u}}^{n}}{2}, \frac{\widetilde{\mathbf{u}}^{n+1} + \widetilde{\mathbf{u}}^{n}}{2}, \mathbf{v} \right)_{\Omega_{t^{n+\frac{1}{2}}}} \\
& - \left(\frac{\widetilde{\mathbf{u}}^{n+1} + \widetilde{\mathbf{u}}^{n}}{2} (\nabla \cdot \mathbf{w}^{n+\frac{1}{2}}), \mathbf{v} \right)_{\Omega_{t^{n+\frac{1}{2}}}} - \left(\mathbf{w}^{n+\frac{1}{2}} \cdot \nabla \frac{\widetilde{\mathbf{u}}^{n+1} + \widetilde{\mathbf{u}}^{n}}{2}, \mathbf{v} \right)_{\Omega_{t^{n+\frac{1}{2}}}} \\
& + \left(\frac{\widetilde{\mathbf{u}}^{n+1} + \widetilde{\mathbf{u}}^{n}}{2} \cdot \nabla \mathbf{u}^{*n+\frac{1}{2}}, \mathbf{v} \right)_{\Omega_{t^{n+\frac{1}{2}}}} + \left(\mathbf{u}^{*n+\frac{1}{2}} \cdot \nabla \frac{\widetilde{\mathbf{u}}^{n+1} + \widetilde{\mathbf{u}}^{n}}{2}, \mathbf{v} \right)_{\Omega_{t^{n+\frac{1}{2}}}} \Bigg] \\
& + \Delta t \Bigg[2(1-\alpha) \left(D\left(\frac{\widetilde{\mathbf{u}}^{n+1} + \widetilde{\mathbf{u}}^{n}}{2} \right), D(\mathbf{v}) \right)_{\Omega_{t^{n+\frac{1}{2}}}} + \left(\frac{\boldsymbol{\sigma}^{n+1} + \boldsymbol{\sigma}^{n}}{2}, D(\mathbf{v}) \right)_{\Omega_{t^{n+\frac{1}{2}}}} \\
& \qquad + (p^{n+1}, \nabla \cdot \mathbf{v})_{\Omega_{t^{n+\frac{1}{2}}}} \Bigg] \\
& = \Delta t \Bigg[(\mathbf{f}^{n+\frac{1}{2}}, \mathbf{v})_{\Omega_{t^{n+\frac{1}{2}}}} - \rho \left(\frac{\partial \mathbf{u}^{*\,n+\frac{1}{2}}}{\partial t} \Big|_{\mathbf{y}} + (\mathbf{u}^{*n+\frac{1}{2}} - \mathbf{w}^{n+\frac{1}{2}}) \cdot \nabla \mathbf{u}^{*n+\frac{1}{2}}, \mathbf{v} \right)_{\Omega_{t^{n+\frac{1}{2}}}} \\
& \qquad - 2(1-\alpha)(D(\mathbf{u}^{*n+\frac{1}{2}}), D(\mathbf{v}))_{\Omega_{t^{n+\frac{1}{2}}}} \Bigg] \quad \forall \mathbf{v} \in \mathbf{U}_{h,t}\,,
\end{aligned}
$$

$$
(4.15) \qquad \left(q, \nabla \cdot \frac{\widetilde{\mathbf{u}}^{n+1} + \widetilde{\mathbf{u}}^{n}}{2} \right)_{\Omega_{t^{n+\frac{1}{2}}}} = 0 \quad \forall q \in Q_{h,t}\,.
$$

ETNA
Kent State University
http://etna.math.kent.edu

A conditional stability result for Algorithm 4.4 is obtained by the same approach as in the proof of Theorem 4.3. The discretized time derivative terms can be estimated as shown in [32] for the Navier-Stokes equation. We present the result without a proof.

THEOREM 4.5. *A solution to the fully discretized system* (4.13)–(4.15) *satisfies the inequality*

$$
\begin{aligned}
&\lambda\|\boldsymbol{\sigma}^{n+1}\|^2_{0,\Omega_{t^{n+1}}} + 2\alpha\rho\|\widetilde{\mathbf{u}}^{n+1}\|^2_{1,\Omega_{t^{n+1}}} \\
&+\Delta t\sum_{i=0}^{n}\left[2\alpha(1-\alpha)C_p^2\|\widetilde{\mathbf{u}}^{i+1}+\widetilde{\mathbf{u}}^{i}\|^2_{1,\Omega_{t^{i+\frac12}}} + \frac{1-4\lambda M}{2}\|\boldsymbol{\sigma}^{i+1}+\boldsymbol{\sigma}^{i}\|^2_{0,\Omega_{t^{i+\frac12}}}\right] \\
&+\Delta t\sum_{i=0}^{n}\left[\frac{\lambda}{4}\int_{\Gamma_{t^{i+\frac12}}}((\mathbf{u}^{*i+1}-\mathbf{w}^{i+\frac12})\cdot\mathbf{n})|\boldsymbol{\sigma}^{i+1}+\boldsymbol{\sigma}^{i}|^2\,d\Gamma_{t^{i+\frac12}}\right. \\
&\left.-\int_{\Omega_{t^{i+\frac12}}}(\nabla\cdot\mathbf{w}^{i+\frac12})\left(\frac{\lambda}{4}|\boldsymbol{\sigma}^{i+1}-\boldsymbol{\sigma}^{i}|^2+\frac{\alpha\rho}{2}|\widetilde{\mathbf{u}}^{i+1}-\widetilde{\mathbf{u}}^{i}|^2\right)d\Omega_{t^{i+\frac12}}\right] \\
&\le \lambda\|\boldsymbol{\sigma}^{0}\|^2_{0,\Omega_0}+2\alpha\rho\|\widetilde{\mathbf{u}}^{0}\|^2_{1,\Omega_0}+C\,\Delta t\sum_{i=0}^{n}\left[\|\mathbf{f}^{i+\frac12}\|^2_{-1,\Omega_{t^{i+\frac12}}}+\left\|\frac{\partial\mathbf{u}^{*\,i+\frac12}}{\partial t}\right\|^2_{by,0,\Omega_{t^{i+\frac12}}}\right. \\
&\qquad\left.+\|\mathbf{u}^{*i+\frac12}\|^4_{1,\Omega_{t^{i+\frac12}}}+\|\mathbf{u}^{*i+\frac12}\|^2_{1,\Omega_{t^{i+\frac12}}}\right].
\end{aligned}
$$

5. Numerical results. In this section we present numerical results of two experiments for the model equations

$$
\begin{aligned}
\boldsymbol{\sigma}+\lambda\left(\frac{\partial\boldsymbol{\sigma}}{\partial t}+\mathbf{u}\cdot\nabla\boldsymbol{\sigma}+g_a(\boldsymbol{\sigma},\nabla\mathbf{u})\right)-2\,\alpha\,D(\mathbf{u})&=\mathbf{f}_1 \quad \text{in } \Omega_t\,,\\
\rho\left(\frac{\partial\mathbf{u}}{\partial t}+\mathbf{u}\cdot\nabla\mathbf{u}\right)-\nabla\cdot\boldsymbol{\sigma}-2(1-\alpha)\,\nabla\cdot D(\mathbf{u})+\nabla p&=\mathbf{f}_2 \quad \text{in } \Omega_t\,,\\
div\ \mathbf{u}&=0 \quad \text{in } \Omega_t\,.
\end{aligned}
\tag{5.1}
$$

Although the model equations were analyzed with the linearized g_a term in (5.1) and the homogeneous stress boundary condition was assumed to simplify the analysis, we approximated the model equations in the standard setting without such simplifications.

The first experiment is to investigate convergence of algorithms with decreasing grid sizes and time steps. The second experiment is designed to test stability of the algorithms.

Experiment 1. Numerical experiments were performed using a non-physical example problem with a known exact solution. The initial domain is chosen as $\Omega_0=\{\mathbf{y}:\mathbf{y}\in[0,1]\times[0,1]\}$ at $t=0$ and the domain thereafter is defined by

$$
\Omega_t=\{\mathbf{x}: x_1=y_1\,(2-\cos(\pi t)),\ x_2=y_2\,(2-\cos(\pi t)) \text{ for } \mathbf{y}\in\Omega_0\}. \tag{5.2}
$$

Using the parameters $\lambda=0.5$, $\alpha=0.5$, $a=0$, the right hand side functions $\mathbf{f}_1$, $\mathbf{f}_2$ were

ETNA
Kent State University
http://etna.math.kent.edu

appropriately given so that the exact solution is

$$\begin{cases} \mathbf{u} = \begin{bmatrix} 10\sin(2\pi t+1)x_1^2(x_1-1)^2x_2(2x_2-1)(x_2-1) \\ -10\sin(2\pi t+2)x_2^2(x_2-1)^2x_1(2x_1-1)(x_1-1) \end{bmatrix} \\ p = \sin(\pi t+2)\cos(2\pi x_1)x_2(x_2-1) \\ \boldsymbol{\sigma} = \begin{bmatrix} \sigma_{11} & \sigma_{12} \\ \sigma_{21} & \sigma_{22} \end{bmatrix} \end{cases}$$

in the initial domain, where $\sigma_{11} = 10\sin(2\pi t+1)x_1^2(x_1-1)^2x_2(2x_2-1)(x_2-1)$, $\sigma_{12} = \sigma_{21} = -10\sin(2\pi t+2)x_2^2(x_2-1)^2x_1(2x_1-1)(x_1-1)$ and $\sigma_{22} = 0$. To approximate the flow equations, we used the Taylor-Hood pair for $(\mathbf{u}, p)$ and discontinuous piecewise linear elements for $\boldsymbol{\sigma}$. Since the domain is defined by (5.2), we used the exact ALE mapping. The exact domain velocity given by

$$\mathbf{w} = \left[\frac{x_1\pi\sin(\pi t)}{2-\cos(\pi t)}, \frac{x_2\pi\sin(\pi t)}{2-\cos(\pi t)}\right]^T. \tag{5.3}$$

In the first test, we computed the L^2, H^1 errors of velocity, and the L^2 error of stress using the fixed number of elements generated by a 26×26 uniform grid and various time steps $\Delta t = \frac{1}{2.5}, \frac{1}{5}, \frac{1}{10}, \frac{1}{15}, \frac{1}{20}, \frac{1}{30}$. With the number of elements chosen, we expected the errors to be dominated by the time step when large Δt values are used. Results by Algorithm 4.2 and Algorithm 4.4 are summarized in Table 5.1 and Table 5.2, respectively. Errors calculated by Algorithm 4.2 converge superlinearly, and the convergence rates for Algorithm 4.4 are higher than for Algorithm 4.2 (as expected). The L^2 errors of the velocity show quadratic convergence.

In the second test we computed velocity and stress errors for various grid sizes with a small fixed Δt so that the finite element discretization error dominates the total error. The errors computed on different meshes using $\Delta t = \frac{1}{2000}$ are presented in Table 5.3 and Table 5.4. Baranger and Sandri [2] derived the finite element error estimate for the model equations in a fixed domain as

$$\|\boldsymbol{\sigma} - \boldsymbol{\sigma}_h\|_0 + \|D(\mathbf{u}) - D(\mathbf{u}_h)\|_0 \le C\,h^{3/2},$$

for the $(P_2, P_1, P_{1\,DG})$ (Taylor-Hood, discontinuous linear) elements.

TABLE 5.1
Errors of velocity and stress by Algorithm 4.2 for $t = 0.4$.

	velocity				stress	
Δt	L^2 error	L^2 rate	H^1 error	H^1 rate	L^2 error	L^2 rate
$1/2.5$	$.1090\cdot 10^{-2}$		$.4877\cdot 10^{-2}$		$.1310\cdot 10^{-2}$	
$1/5$	$.5140\cdot 10^{-3}$	1.11	$.1974\cdot 10^{-2}$	1.30	$.5539\cdot 10^{-3}$	1.24
$1/10$	$.1820\cdot 10^{-3}$	1.50	$.6523\cdot 10^{-3}$	1.30	$.1683\cdot 10^{-3}$	1.72
$1/15$	$.1019\cdot 10^{-3}$	1.43	$.3801\cdot 10^{-3}$	1.33	$.9393\cdot 10^{-4}$	1.44
$1/20$	$.6905\cdot 10^{-4}$	1.35	$.2673\cdot 10^{-3}$	1.22	$.6404\cdot 10^{-4}$	1.33
$1/30$	$.4114\cdot 10^{-4}$	1.28	$.1670\cdot 10^{-3}$	1.16	$.3822\cdot 10^{-4}$	1.27

Experiment 2. In this experiment we investigated the numerical stability of Algorithm 4.2 and Algorithm 4.4. In this test, a nonzero initial velocity $\mathbf{u}$ and stress $\boldsymbol{\sigma}$ are prescribed (at $t = 0$), and the right-hand side functions $\mathbf{f}_1, \mathbf{f}_2$ of the equations are set to $\mathbf{0}$, and the moving domain boundary is assumed to follow the same specification as given in Experiment 1 (5.3).

ETNA
Kent State University
http://etna.math.kent.edu

TABLE 5.2
Errors of velocity and stress by Algorithm 4.4 for $t = 0.4$.

	velocity				stress	
Δt	L^2 error	L^2 rate	H^1 error	H^1 rate	L^2 error	L^2 rate
$1/2.5$	$.1312 \cdot 10^{-2}$		$.5575 \cdot 10^{-2}$		$.1706 \cdot 10^{-2}$	
$1/5$	$.3172 \cdot 10^{-3}$	2.05	$.1638 \cdot 10^{-2}$	1.77	$.6081 \cdot 10^{-3}$	1.48
$1/10$	$.6250 \cdot 10^{-4}$	2.34	$.2798 \cdot 10^{-3}$	2.55	$.1300 \cdot 10^{-3}$	2.23
$1/15$	$.2674 \cdot 10^{-4}$	2.09	$.1437 \cdot 10^{-3}$	1.64	$.5559 \cdot 10^{-4}$	2.10
$1/20$	$.1490 \cdot 10^{-4}$	2.03	$.9515 \cdot 10^{-4}$	1.44	$.3380 \cdot 10^{-4}$	1.73
$1/30$	$.6783 \cdot 10^{-5}$	1.94	$.5815 \cdot 10^{-4}$	1.21	$.2872 \cdot 10^{-4}$	0.40

TABLE 5.3
Errors of velocity and stress by Algorithm 4.2 for $t = 0.2$.

	velocity				stress	
grid	L^2 error	L^2 rate	H^1 error	H^1 rate	L^2 error	L^2 rate
3×3	$.2645 \cdot 10^{-4}$		$.3244 \cdot 10^{-3}$		$.2853 \cdot 10^{-3}$	
5×5	$.8043 \cdot 10^{-5}$	1.72	$.1291 \cdot 10^{-3}$	1.33	$.8307 \cdot 10^{-4}$	1.78
9×9	$.1859 \cdot 10^{-5}$	2.11	$.2477 \cdot 10^{-4}$	2.38	$.1960 \cdot 10^{-4}$	2.08
13×13	$.1139 \cdot 10^{-5}$	1.21	$.1112 \cdot 10^{-4}$	1.98	$.8538 \cdot 10^{-5}$	2.05
17×17	$.9111 \cdot 10^{-6}$	.78	$.7286 \cdot 10^{-5}$	1.47	$.4681 \cdot 10^{-5}$	2.09

TABLE 5.4
Errors of velocity and stress by Algorithm 4.4 for $t = 0.2$.

	velocity				stress	
grid	L^2 error	L^2 rate	H^1 error	H^1 rate	L^2 error	L^2 rate
3×3	$.2778 \cdot 10^{-4}$		$.3483 \cdot 10^{-3}$		$.3413 \cdot 10^{-3}$	
5×5	$.9417 \cdot 10^{-5}$	1.56	$.1570 \cdot 10^{-3}$	1.15	$.1006 \cdot 10^{-3}$	1.76
9×9	$.1455 \cdot 10^{-5}$	2.69	$.2544 \cdot 10^{-4}$	2.63	$.2172 \cdot 10^{-4}$	2.21
13×13	$.6049 \cdot 10^{-6}$	2.16	$.1230 \cdot 10^{-4}$	1.79	$.1002 \cdot 10^{-4}$	1.91
17×17	$.3916 \cdot 10^{-6}$	1.51	$.6256 \cdot 10^{-5}$	2.35	$.6734 \cdot 10^{-5}$	1.38

If $\alpha \neq 1$ and if λ and M are not too large (as required by Theorems 4.3 and 4.5), as time proceeds beyond the initial value, the solution components $\mathbf{u}$ and $\boldsymbol{\sigma}$ are expected to decay, eventually leading to $\|\mathbf{u}\|_{1,\Omega_t} = \|\boldsymbol{\sigma}\|_{0,\Omega_t} = 0$. Provided the algorithms presented in Section 4 are stable, the computed approximations should decay as well. The divergence-free initial velocity, shown in Figure 5.1, is given by

$$\mathbf{u} = \begin{bmatrix} 10(x_1^4 - 2x_1^3 + x_1^2)(2x_2^3 - 3x_2^2 + x_2) \\ -10(2x_1^3 - 3x_1^2 + x_1)(x_2^4 - 2x_2^3 + x_2^2) \end{bmatrix},$$

the initial stress is $\boldsymbol{\sigma} = 2\alpha D(\mathbf{u})$, and the initial pressure is $p = 0$. We use the parameter values $a = 0$ and $\alpha = 0.5$. Computations were performed on a uniform mesh with initial width $h = 1/8$ and time-step $\Delta t = 0.025$ for the values $\lambda = 0.1$ and $\lambda = 1.0$, and were allowed to continue until the norms $\|\mathbf{u}\|_{1,\Omega_t}$ and $\|\boldsymbol{\sigma}\|_{0,\Omega_t}$ were sufficiently small. A plot of these norms of solution components as time progresses is given for each value of λ in Figures 5.2 and 5.3, respectively. As is observed in the plots, the computed approximations do decay for both methods. Note that for larger λ the numerical stability degrades, due to the fact that the hypothesis $1 - 4M\lambda > 0$ of Theorems 4.3 and 4.5 is violated, as $M \geq \|\nabla \mathbf{u}_0\|_\infty = 0.625$.

ETNA
Kent State University
http://etna.math.kent.edu

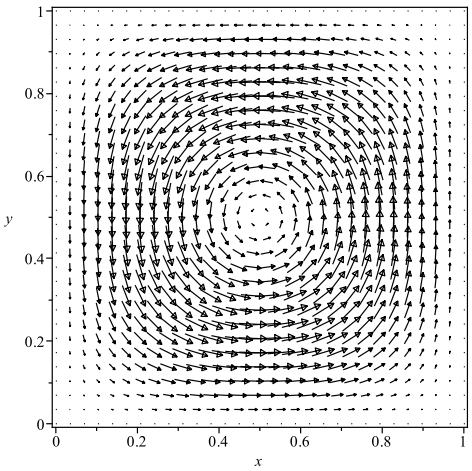

FIG. 5.1. *Initial velocity profile, Experiment 2.*

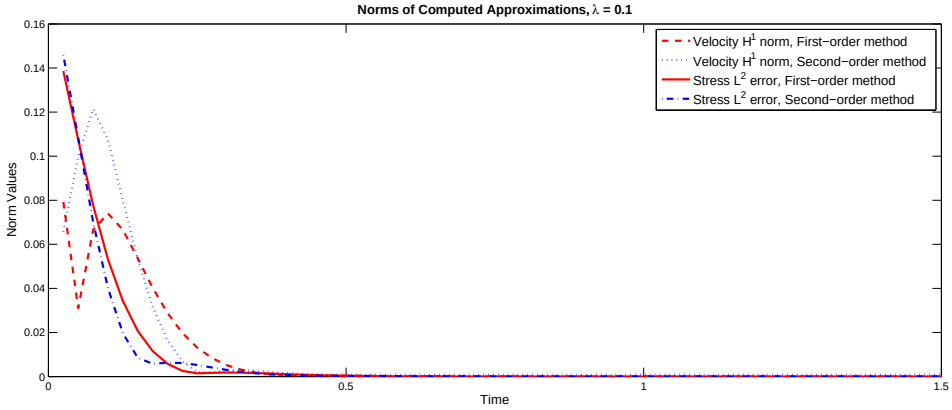

FIG. 5.2. *Norms of computed approximations,* $\lambda = 0.1$.

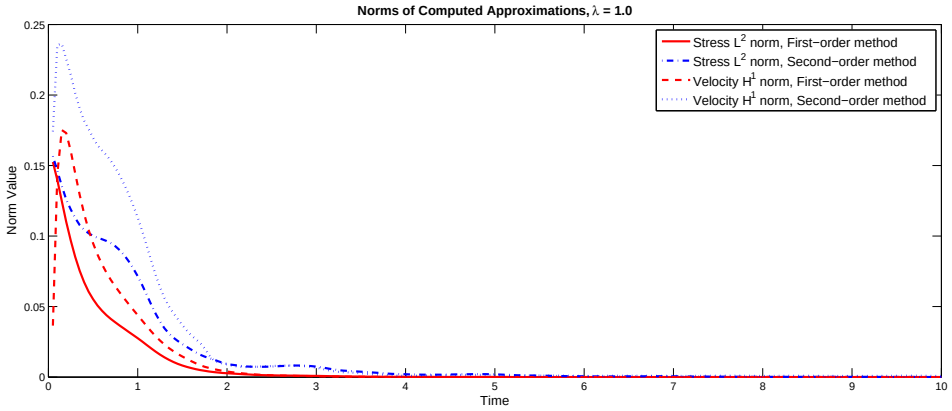

FIG. 5.3. *Norms of computed approximations,* $\lambda = 1.0$.

ETNA
Kent State University
http://etna.math.kent.edu

6. Concluding remarks. We have presented a rigorous stability analysis of a finite element method for the ALE formulation of viscoelastic flows in a moving domain. There have been numerical results reported on viscoelastic flows in deformable domains or fluids coupled with elastic solids. However, there are few analytical studies in literature for such problems. This is our initial effort towards an analytical and numerical study of viscoelastic flows in an elastic solid structure. Our numerical tests support the analytical stability results, and suggest that the mesh convergence result for a fixed domain problem may still hold in the case of moving domain problems. Subsequent work will further develop the fluid-structure interaction model and include numerical experiments that are designed to determine if the fluid model significantly affects the behavior of the coupled system.

REFERENCES

[1] S. BADIA AND R. CODINA, *Analysis of a stabilized finite element approximation of the transient convection-diffusion equation using an ALE framework,* SIAM J. Numer. Anal., 44 (2006), pp. 2159–2197.
[2] J. BARANGER AND D. SANDRI, *Finite element approximation of viscoelastic fluid flow: existence of approximate solutions and error bounds I. Discontinuous constraints*, Numer. Math, 63 (1992), pp. 13–27.
[3] T. BODNÁR AND A. SEQUEIRA, *Numerical study of the significance of the non-Netwonian nature of blood in steady flow through a stenosed vessel*, in Advances in Mathematical Fluid Mechanics. Selected Papers from the International Conference on Mathematical Fluid Mechanics held in Estoril, May 2007, R. Rannacher and A. Sequeira, eds., Springer, Berlin, 2010, pp. 83–104.
[4] T. BODNÁR, A. SEQUEIRA, AND M. PROSI, *On the shear-thinning and viscoelastic effects of blood flow under various flow rates*, Appl. Math. Comput., 217 (2011), pp. 5055–5067.
[5] D. BOFFI AND L. GASTALDI, *Stability and geometric conservation laws for ALE formulations*, Comput. Methods. Appl. Mech. Engrg., 193 (2004), pp. 4717–4739.
[6] S. BRENNER AND L. SCOTT, *The Mathematical Theory of Finite Element Methods*, Springer, New York, 1994.
[7] P. CAUSIN, J-F. GERBEAU, AND F. NOBILE, *Added-mass effect in the design of partitioned algorithms for fluid-structure problems*, Comput. Methods Appl. Mech. Engrg., 194 (2005), pp. 4506–4527.
[8] S. CANIĆ, A. MIKELIĆ, AND J. TAMBAČA, *Two dimensional effective model describing fluid-structure interaction in blood flow: analysis, simulation and experimental validation*, C. R. Mecanique, 333 (2005), pp. 867–883.
[9] J. C. CHRISPELL AND L. J. FAUCI, *Peristaltic pumping of solid particles immersed in a viscoelastic fluid*, Math. Model. Nat. Phenom, 6 (2011), pp. 67–83.
[10] S. DEPARIS, M. A. FERNÁNDEZ, L. FORMAGGIA, AND F. NOBILE, *Modified fixed point algorithm in fluid-structure interaction*, C. R. Mecanique, 331 (2003), pp. 525–530.
[11] J. DONEA, S. GIULIANI, AND J. P. HALLEUX, *An arbitrary Lagrangian-Eulerian finite element method for transient dynamic fluid-structure interactions*, Comput. Methods Appl. Mech. Engrg., 33 (1982), pp. 689–723.
[12] V. J. ERVIN, H. K. LEE, AND L. N. NTASIN, *Analysis of the Oseen-viscoelastic fluid flow problem*, J. Non-Newtonian Fluid Mech., 127 (2005), pp. 157–168.
[13] L. FORMAGGIA, J.F. GERBEAU, F. NOBILE, AND A. QUARTERONI, *On the coupling of 3D and 1D Navier-Stokes equations for flow problems in compliant vessels*, Comput. Methods Appl. Mech. Engrg., 191 (2001), pp. 561–582.
[14] L. FORMAGGIA, A. MOURA, AND F. NOBILE, *On the stability of the coupling of 3D and 1D fluid-structure interaction models for blood flow simulations,* M2AN Math. Mod. Numer. Anal., 41 (2007), pp. 743–769.
[15] L. FORMAGGIA AND F. NOBILE, *A stability analysis for the arbitrary Lagrangian Eulerian formulation with finite elements*, East-West J. Numer. Math., 7 (1999), pp. 105–131.
[16] ———, *Stability analysis of second-order time accurate schemes for ALE-FEM*, Comput. Methods. Appl. Mech. Engrg., 193 (2004), pp. 4097–4116.
[17] L. FORMAGGIA, A. QUARTERONI, AND A. VENEZIANI, eds., *Cardiovascular Mathematics*, Springer, Milano, 2009.
[18] A. FORTIN AND A. ZINE, *An improved GMRES method for solving viscoelastic fluid flow problems*, J. Non-Newtonian Fluid Mech., 42 (1992), pp. 1–18.
[19] M.A. FERNÁNDEZ, J. F. GERBEAU, AND C. GRANDMONT, *A projection semi-implicit scheme for the coupling of an elastic structure with an incompressible fluid*, Internat. J. Numer. Meth. Engng., 69 (2007), pp. 794–821.
[20] G. P. GALDI, R. RANNACHER, A. M. ROBERTSON, AND S. TUREK, eds., *Hemodynamical flows*, vol. 37 of

ETNA
Kent State University
http://etna.math.kent.edu

Oberwolfach Seminars, Birkhäuser Verlag, Basel, 2008.
[21] L. GASTALDI, *A priori error estimates for the arbitrary Lagrangian Eulerian formulation with finite elements*, East-West J. Numer. Math., 9 (2001), pp. 123–156.
[22] V. GIRAULT AND P. RAVIART, *Finite Element Methods for Navier-Stokes Equations*, Springer, Berlin, 1986.
[23] H. GUILLARD AND C. FARHAT, *On the significance of the geometric conservation law for flow computations on moving meshes*, Comput. Methods Appl. Mech. Engrg., 190 (2000), pp. 1467–1482.
[24] T. J. R. HUGHES, W. K. LIU, AND T. K. ZIMMERMANN, *Lagrangian-Eulerian finite element formulation for incompressible viscous flows*, Comput. Methods Appl. Mech. Engrg., 29 (1981), pp. 329–349.
[25] J. JANELA, A. MOURA, AND A. SEQUEIRA, *A 3D non-Newtonian fluidstructure interaction model for blood flow in arteries*, J. Comput. Appl. Math., 234 (2010), pp. 2783–2791.
[26] W. LAYTON, *Introduction to the Numerical Analysis of Incompressible Viscous Flows*, SIAM, Philadelphia, 2008.
[27] H. LEE, *Numerical approximation of quasi-Newtonian flows by ALE-FEM*, Numer. Methods Partial Differential Equations, 28 (2012), pp. 1667–1695.
[28] P. LETALLEC AND S. MANI, *Numerical analysis of a linearized fluid-structure interaction problem*, Numer. Math., 87 (2000), pp. 317–354.
[29] M. LUKÁČOVÁ-MEDVIĎOVÁ AND A. ZAUŠKOZÁ, *Numerical modelling of shear-thinning non-Newtonian flows in compliant vessels*, Internat. J. Numer. Methods Fluids, 56 (2008), pp. 1409–1415.
[30] J. S. MARTIN, L. SMARANDA, AND T. TAKAHASHI, *Convergence of finite element/ALE method for the Stokes equations in a domain depending on time*, J. Comput. Appl. Math., 230 (2009), pp. 521–545.
[31] L. NADAU AND A. SEQUEIRA, *Numerical simulations of shear dependent viscoelastic flows with a combined finite element–finite volume method*. Comput. Math. Appl., 53 (2007), pp. 547–568.
[32] F. NOBILE, *Numerical Approximation of Fluid-Structure Interaction Problems with Application to Haemodynamics*, Ph.D. Thesis, École Polytechnique Fédérale de Lausanne, Lausanne, Switzerland, 2001.
[33] F. NOBILE AND C. VERGARA, *An effective fluid-structure interaction formulation for vascular dynamics by generalized Robin conditions*, SIAM J. Sci. Comp., 30 (2008), pp. 731–763.
[34] A. QUARTERONI AND L. FORMAGGIA, *Mathematical modelling and numerical simulation of the cardiovascular system*, in Computational Models for the Human Body, N. Ayache, ed., Handbook of Numerical Analysis 12, Elsevier, Amsterdam, 2004, pp. 3–127.
[35] A. QUARTERONI, M. TUVERI, AND A. VENEZIANI, *Computational vascular fluid dynamics: problems, models, and methods*, Comput. Visual Sci., 2 (2000), pp. 163–197.
[36] O. REYNOLDS, *Papers on Mechanical and Physical Subjects Vol. I*, The University Press, Cambridge, 1900.
[37] C. A. TAYLOR, T. J. R. HUGHES, AND C. K. ZARINS, *Finite element modeling of blood flow in arteries*, Comput. Methods. Appl. Mech. Engrg., 158 (1998), pp. 155–196.
[38] R. TEMAM, *Navier-Stokes Equations. Theory and Numerical Analysis*, AMS Chelsea Publishing, 1984.
[39] J. TERAN, L. FAUCI, AND M. SHELLEY, *Peristaltic pumping and irreversibility of a Stokesian viscoelastic fluid*, Phys. Fluids, 20 (2008), 073101, (11 pages).
[40] R. TORII, M. OSHIMA, T. KOBAYASHI, K. TAKAGI, AND T. F. TEZDUYAR, *Computer modeling of cardiovascular fluid-structure interactions with the deforming-spatial-domain/stabilized space-time formulation*, Comput. Methods. Appl. Mech. Engrg., 195 (2006), pp. 1885–1895.
[41] K. K. YELESWARAPU, *Evaluation of Continuum Models for Characterizing the Constitutive Behavior of Blood*, Ph.D. Thesis, University of Pittsburgh, Pittsburgh, 1996.